THE ASTROPHYSICAL JOURNAL, 346:303–329, 1989 November 1

THE EVOLUTION OF CHROMOSPHERIC ACTIVITY OF COOL GIANT AND SUBGIANT STARS

THEODORE SIMON[1,2]
Laboratory for Astronomy and Solar Physics, NASA/Goddard Space Flight Center
AND
STEPHEN A. DRAKE[1,2]
ST Systems Corporation
Received 1988 December 26; accepted 1989 April 28

ABSTRACT

From an examination of *IUE* spectra for a large sample of cool subgiant stars, we have found evidence that subgiants in the mass range 1.2–1.6 $M_\odot$ undergo a sudden decline in UV transition region emission near $B-V = 0.6$, which corresponds to spectral type G0 IV. The evolutionary time scale for this decline is on the order of 100 Myr, or less. The decline in UV emission coincides with a sharp decrease in stellar rotation rates. We suggest that this decay in activity and rotation marks a transformation from acoustic heating in the early F stars to magnetic dynamo-driven activity in the cooler stars, a primary result of which is to induce a strong rotational braking action by means of a stellar wind.

For more massive giant stars, there is a similar transformation in the nature of chromospheric (and coronal) activity near $B-V = 0.7$, or spectral type G0 III, from acoustic heating in the F-type giants (including the archetypal active chromosphere star, Capella Ab) to a solarlike dynamo mechanism in the cooler giants. We see no sign of an abrupt drop in activity near spectral type G5 III at the location of Gray's proposed rotational boundary line. Thus, we cannot tell whether stars evolving through the Hertzsprung gap conserve angular momentum or whether they require an external rotational brake to explain their decay in activity and rotation. The ultrarapid rotation of some apparently single, first-crossing, early K giants is attributed to a sudden dredge-up of angular momentum from the interior.

We find evidence that the soft X-ray emission of the early F stars, from dwarfs to giants, is weak relative to that of the solar-type stars, and we tentatively suggest that these stellar coronae are expanding outward in massive coronal winds. A definitive test of this idea could be provided by observations of Doppler shifts in the UV coronal lines of Fe XII from the Hubble Space Telescope.

Subject headings: stars: chromospheres — stars: evolution — stars: late-type — stars: rotation — ultraviolet: spectra

I. INTRODUCTION

Throughout their main-sequence lifetimes, low-mass stars undergo a systematic decline in their rotation speed and in their chromospheric emission. Thus, on average, solar-type stars in the field rotate much more slowly than their counterparts in young clusters and display much less intense chromospheric emission (Wilson 1963; Kraft 1967; Skumanich 1972; Soderblom 1983; Simon, Herbig, and Boesgaard 1985). In the very broadest sense (since many of the observational and theoretical details are not completely agreed upon), this evolution of rotation and chromospheric activity can be understood in terms of the dynamo model for rotating, convective stars. In the dynamo model, surface activity is the result of the interaction of magnetic fields with rotation and convection, either within the convection zone itself or within a shear zone located between the convection zone and the underlying radiative core of the star (Gilman 1983; Glatzmaier 1985; Gilman and DeLuca 1986). The strength of the dynamo is therefore expected to depend on the speed at which a star rotates, and indeed, for main-sequence stars later than about F5, there is now considerable evidence for such a correlation (Noyes *et al.* 1984; Simon, Herbig, and Boesgaard 1985, hereafter SHB; Simon and Fekel 1987). In a way that has as yet found no generally accepted explanation, the dynamo process also leads to the formation of a coronal wind, which is coupled to the star by means of a large-scale magnetic field. The magnetic torque exerted by the wind acts to decelerate the star (Weber and Davis 1967; Kraft 1967), so that by the end of its main-sequence existence a solar-type star is likely to be both a very slow rotator and a very weak chromospheric and coronal emitter.

One then might ask, how does this activity change during the subsequent phase of evolution, once a star leaves the main sequence and becomes a subgiant? Does it diminish further, or does it intensify as the convection zone starts to grow in size? Based upon a consideration of the magnitude of the dynamo number, which is related to the thickness of the convection zone, Gilliland (1985*a*) has predicted that the activity of low-mass stars should increase once they leave the main sequence. On the other hand, Gray and Nagar (1985) have observed a sharp decline in the rotation speeds of subgiant stars near G0 IV, just at the point where the convective envelope starts to grow very rapidly, which they have attributed to the activation of a dynamo magnetic brake. Since this spin-down could inhibit a star's ability to sustain a vigorous dynamo, Gray and Nagar have predicted a decline in chromospheric activity at that point. Unfortunately, although chromospheric emission in

[1] Guest Observer with the *International Ultraviolet Explorer* (*IUE*) satellite.
[2] Guest Investigator with the *Einstein Observatory* (*HEAO 2*).

the Ca II H and K lines is nearly universal among the coolest subgiants and giants, there have been few if any quantitative studies of the absolute flux of chromospheric emission within this region of the H-R diagram (e.g., Wilson 1968, 1982). Neither have any previous studies of the UV chromospheric lines been extensive enough to test these two conflicting predictions.

A similar question arises in connection with the post–main-sequence evolution of stars that are much more massive than the Sun. On the main sequence, B- and early A-type stars lack surface convection zones, they show none of the obvious signs of chromospheres, and their rotation rates are typically much faster than those of low-mass stars like the Sun. After these stars evolve off the main sequence and enter the Hertzsprung gap, how does their activity change once they begin to develop substantial convection zones?

For the Ca II H and K lines this last question was investigated by Wilson (1982) and by Rutten and Pylyser (1988), and for the UV chromospheric lines it was investigated by Simon (1984). Observations of luminosity class III giants reveal a systematic decline in the strengths of the Ca II H and K emission and of the transition region lines of C II and C IV with increasing $B-V$. From very high values among the F–G yellow giants, the emission falls to very low levels near $B-V = 1.0$, at the point dividing the yellow giants from the red giants.

This decrease in activity across the Hertzsprung gap is matched by a drop in the rotation rates of late-type giants (Kraft 1970). What has not been determined so far is whether angular momentum is conserved as stars evolve through this region of the H-R diagram, or whether an external rotational brake is needed. The resolution of this issue has remained clouded by the lack of good stellar evolutionary models that include rotation (see, however, Endal and Sofia 1979) and by a dearth of rotational velocities for the generally slowly rotating G and K giants. The latter deficiency has been remedied, in part, by Gray (1982*a*), who claims to find an abrupt decrease in rotation rates near G5 III. Endal (1981) has shown that evolutionary models that conserve angular momentum cannot account for this sudden drop in velocity, but if a magnetic brake is imposed, as Gray has argued, then field strengths of several tens of gauss are needed to spin the giant stars down on evolutionary time scales of only 5–10 Myr. One might therefore inquire whether this rotational discontinuity is also reflected in the strength of the chromospheric emission of these stars as they pass through the Hertzsprung gap.

Finally, one can speculate about changes in the activity of stars of intermediate mass, 1.2–1.5 $M_\odot$, once they evolve off the main sequence from the vicinity of the late A or early F stars to become cool subgiants. In the past, when the Ca II H and K emission reversals were the only chromospheric indicators available and emission was undetected among the late A and early F stars, the convection zones of these stars were thought to be too thin to support chromospheres and coronae (Wilson 1966). However, it is now known from X-ray observations obtained by the *Einstein* satellite (Schmitt *et al.* 1985*a*) and from UV observations made by *IUE* (Wolff, Boesgaard, and Simon 1986, hereafter WBS; Simon and Landsman 1987) that these stars have very strong chromospheres and coronae, despite their thin convection zones. Therefore, the absence of Ca II emission in the spectra of stars earlier than ~F5 V is most likely only an artifact caused by a loss of contrast against a bright photospheric spectrum at 3950 Å.

These recent studies also indicate that the activity of the main-sequence stars earlier than F5 may be independent of their rotation rate (WBS; Walter 1983). The activity of the early stars may therefore be produced in a fundamentally different way than the dynamo-generated activity of the cooler stars. Durney and Latour (1978), it should be noted, claimed that the convection zones of the A and early F stars are too thin to support efficient dynamos; that the *e*-folding time for magnetic braking of these stars is >1000 times longer than the solar spin-down time (which is of order 1 Gyr: Pizzo *et al.* 1983); and that, as a consequence, stars more massive than the Sun can maintain their rapid rotation throughout their entire main-sequence lifetimes. Now, one might ask whether these early-type stars, when they evolve off the main sequence, simply carry their high levels of activity into the subgiant region of the H-R diagram, or whether at some point they develop deep enough convection zones to initiate a strong dynamo and show signs of a correlation between activity and rotation.

In this paper we attempt to address some of these questions concerning the effects of post–main-sequence evolution on the level of chromospheric activity in cool stars. Since late-type subgiants have received scant attention from most previous *IUE* observers, we have obtained *IUE* spectra of a sample of subgiants with masses between 1 and 1.5 $M_\odot$, and we have combined these data with similar data for a number of giant stars in order to examine the same questions in the case of more massive stars.

II. OBSERVATIONS

In this study we have used the short-wavelength (1200–2000 Å) camera of *IUE* to obtain low-dispersion spectra of 10 late-type subgiant stars. Each of the stars has a well-determined parallax from *The Bright Star Catalogue* (Hoffleit and Jaschek 1982). The exposure times of the images ranged from 130 to 240 minutes. For six stars we also made use of the long-wavelength camera (2200–3200 Å) to obtain high-dispersion spectra of the Mg II lines, with exposure times that ranged from 20 to 50 minutes. These new observations were supplemented with a number of additional spectra of such stars, which we obtained from the *IUE* archives.

All of the spectra were calibrated and analyzed with standard computer programs at the Goddard Regional Data Analysis Facility. From the short-wavelength spectra we measured the integrated fluxes, or upper limits to those fluxes, of the strongest chromospheric and transition region lines. To obtain integrated fluxes from the profiles of the Mg II lines, we used the standard echelle grating constants to splice together adjacent orders of the spectrum. Table 1 summarizes the results of our measurements. To add to these data, we have adopted emission-line fluxes for other subgiants and dwarfs from various sources in the literature (SHB; WBS; Simon and Landsman 1987), raising the number of such stars in our sample to 89 in all.

We have combined these data with UV line fluxes for 56 giant stars with spectral types in the range from F2 to K2. Most of the relevant spectra have already appeared in the literature (e.g., Ayres, Marstad, and Linsky 1981; Simon, Linsky, and Stencel 1982; Simon 1984), but 10 of them are unpublished observations from our own *IUE* guest observer programs. Our new flux measurements are listed in Table 2.

In the analysis undertaken here we have chosen to discuss only the C II 1335 Å and C IV 1550 Å emission lines. These two lines are the strongest and most easily measured features in the short-wavelength spectra and, consequently, provide the largest sample of measurements. (The C II line is likely formed in the high chromosphere at temperatures near 15,000 K, while

TABLE 1

LINE FLUXES AT EARTH FOR DWARFS AND SUBGIANTS (10^{-13} ergs cm^{-2} s^{-1})

Star	N V λ1240	O I λ1305	C II λ1335	Si IV λ1400	C IV λ1549	He II λ1640	C I λ1657	Si II λ1810	Mg II λ2800
β Hyi	0.24	2.15	1.32	1 .24	1.80	...	...	...	250.
HR 244	...	<1.20	<1.20	...	<2.00	...	...	...	...
υ^2 Cas		0.80	<0.04	...	...	...	...	0.39	39.0
ρ Psc	1.36	...	2.71	4.28	4.84	...	...	...	...
ν Psc	...	1.51	<0.20		<0.28	...	...	0.52	38.1
χ Eri		4.60	1.80	1.50	2.40	0.88	1.60[a]	>5.70	158.
δ Eri		1.30	1.10	0.46[a]	0.99[a]	<0.17	1.10[a]	2.20	151.
43 Per	0.65	0.52	0.92		0.73[a]	...	...	...	...
ε Ret	...	0.63	0.36	...	<0.88	0.39	...	0.89	46.0
ζ Dor	0.42	1.22	3.54	4.43	7.75	...	...	...	...
HR 2102	0.22	0.94	<0.11	...	<0.11	<0.22	<0.22	0.53[a]	46.3
ν^2 CMa	...	<0.69	<0.69	<1.80	<1.20	...	...	...	82.0
HR 2740	0.89[a]	2.80[a]	3.64	4.80[a]	7.40	...	...	...	...
32 Lyn	...	0.54[a]	1.13	...	2.44	...	...	...	...
69 Vir	...	<0.69	0.11[a]	...	<0.64	<0.09	<0.09	0.71[a]	...
HR 5156	<0.20	0.41	0.40	...	0.51	...	...	...	...
η Boo	0.48[a]	3.66	3.02	1.87	4.52	...	...	...	>220.
12 d Boo	...	<0.44	<0.44	...	<0.44	...	...	...	...
θ Boo	1.00	3.60	7.05	7.67	10.0	2.18	3.81	...	...
16 Lib	...	2.06	3.43	...	5.39	...	...	...	...
14 Oph	0.88	0.59[a]	1.00	0.76[a]	3.00[a]	...	...	...	...
ζHer	...	3.10	3.00	2.20[a]	2.80	...	...	...	...
19 Dra	1.24[a]	0.88	1.84	1.42	...	...	...	...	...
47 Oph	1.86	2.63	4.07	...	5.32	...	...	...	...
μ Her	0.30	0.91	0.97	0.73[a]	1.20	<0.59	1.80	...	...
HR 6670	...	1.08	1.12	...	1.67	0.48	...	...	...
73 Oph	...	<0.95	<0.82	0.90	0.69	...	...	...	...
η Ser	0.16	2.00	0.56	...	0.73	...	0.97	2.00	148.
59 Dra	...	1.54	3.70	3.16	6.71	...	...	...	...
β Aql	...	1.10	0.82	...	<0.55	0.91	1.60	1.40	100.
δ Pav	...	0.90	1.00	...	1.90	...	1.60	2.50	58.0
η Cep	<0.77	0.94[a]	1.29[a]	...	<1.11	...	1.21	2.44	180.
ε Equ	0.86[a]	1.14	2.84	1.60[a]	4.05	...	...	...	78.3
ν Oct	...	1.30	0.37		<0.46	<0.33	...	1.30	>108.
16 Cep	1.19	3.58	4.51	5.12	8.20	...	...	...	...
7 And	1.61	2.40	11.0	5.92	9.00	...	...	...	...
ψ^1 Aqr	<0.36	<0.73	<0.73	<0.30	...	<0.19	<0.19	<0.28	53.3
υ Peg	...	7.90	10.0	7.60	17.0	...	6.30	...	360.
γ Cep	<0.66	2.80	1.40	2.40	2.37	...	2.80	4.00	190.

[a] Uncertain flux.

C IV is formed in the transition region at temperatures near 100,000 K.) The integrated line fluxes are listed in Table 3 for the entire sample of low-luminosity stars and in Table 4 for the high-luminosity stars. For both lines we give the normalized flux, that is, the integrated line flux as a fraction of the apparent bolometric luminosity, l_{bol}, of the star.

Table 3 also gives the absolute visual magnitude of each star, which we calculated from the V-magnitude and the parallax. In general, these M_v values are in very good agreement with the estimates obtained from Strömgren photometry (WBS); in only six cases do the values differ by as much as 0.75 mag. We also tabulate the observed rotation speed $v \sin i$ for each star, where these data are available. The values cited in Table 3 for the early F stars are chiefly from *The Bright Star Catalogue*, while the majority of those listed for solar-type stars are from Soderblom (1983) or Gray (1984). The subgiant rotation rates are from Gray and Nagar (1985) if available, or *The Bright Star Catalogue* otherwise. The rotation rates listed for the giant stars in Table 4 are from *The Bright Star Catalogue*, Danziger and Faber (1972), Alschuler (1975), Gray (1982*a*), and Gray and Toner (1986).

These $v \sin i$ data are plotted as a function of $B-V$ in Figure

TABLE 2

LINE FLUXES AT EARTH FOR GIANTS (10^{-13} ergs cm^{-2} s^{-1})

Star	N V λ1240	O I λ1305	C II λ1335	Si IV λ1400	C IV λ1549	He II λ1640	C I λ1657	Si II λ1810	Mg II λ2800
HD 483	0.19	0.22	0.21	...	0.50[a]	...	1.00	0.94	...
η Psc	0.44	2.30	0.51	...	0.89	0.75	1.40	...	130.
16 Per	1.10	1.70	2.20	1.60[a]	4.00[a]	...	...	...	...
o Tau	...	1.40	<0.10	...	<0.20	<0.60	0.92	1.10	114.
15 Ori	<0.55	<1.50	<2.20	<2.60	5.00[a]	...	...	...	...
HR 1889	0.57	0.83	1.20	1.50	1.80	<0.18	0.80	...	...
45 Aur	0.91	1.40	1.80	2.40	2.20	0.79	0.90	...	...
δ Col	...	0.99	0.09	...	<0.20	0.59	1.30[a]	0.72	78.0
25 Mon	0.49	2.00	2.70	2.40	4.30	0.45	1.70	...	...
o Gem	0.88	1.70	3.10	2.40	4.70	...	...	...	...
o UMa	0.45[a]	2.50	1.60	...	<0.83	0.86	0.95	3.20	150.
35 Cnc	1.10	1.90	1.40	1.50	3.30	0.60[a]	1.00	1.60	...
ι Cnc	0.23[a]	1.50	0.49	0.71[a]	0.71	0.51[a]	0.43	1.20	78.4
27 Hya	...	...	<0.10	...	<0.30	...	...	0.97	...
HR 4529	0.09	...	0.16[a]	...	0.40[a]	0.50[a]	...	...	...
18 Com	1.20	2.50	3.90	3.40	7.80	2.20	...	...	...
γ Hya	1.30	4.30	0.85	...	2.30	0.80	1.30	3.00	210.
δ Boo	...	2.20	0.29	0.66	0.85	0.54	1.00	1.60	150.
84 Her	0.73	0.17[a]	0.14[a]	0.38[a]	0.50	0.76	0.56[a]	0.60[a]	...
θ Her	0.54	>14.3	...	...	<0.46	0.43	2.70	2.70	...
ν Oph	0.54	1.60	0.41	...	<0.30	1.20[a]	1.60[a]	2.50	97.4
δ Dra	0.52	2.50	0.76	...	<0.30	...	1.50	2.70	170.
α Sge	1.60	4.30	1.80	...	<1.60	<1.00	2.20[a]	5.20	...
ε Dra	0.48	1.40	<0.20	...	<0.80	...	0.45[a]	...	100.
HR 7606	...	1.00	0.52[a]	...	<1.00	...	1.30	...	...
ε Cyg	<0.50	5.60	1.30	...	0.69	<0.78	2.00	4.50	294.
HR 8191	0.35	1.20	0.75	1.20	1.20	0.15	0.84	...	...
20 Peg	0.27	0.53	1.10	1.60	1.00	0.80	1.50	...	...
31 Cep	1.80	0.92	1.00	1.60[a]	1.70[a]	1.10	...	...	...
HR 8626	0.17	0.58	0.57	0.70[a]	0.53	...	...	0.87	...
π Cep	3.20	2.50	1.20	2.80	<2.40	...	...	...	...
ω Psc	1.80[a]	4.10	8.90	5.40	11.0	...	...	...	450.

[a] Uncertain flux.

1, the low-luminosity stars in the upper panel and the giant stars in the lower panel. Along the main sequence, rotation rates fall steeply throughout the early F stars; among field stars later than F5 V, rapid rotation, $v \sin i > 50$ km s^{-1}, is rarely observed unless the stars are extremely young or are members of close binaries (Wilson 1966; Kraft 1967).[3]

[3] It is often said, following the conclusions reached by Kraft (1967), that there is a sharp decline in rotation along the main sequence at spectral type F4 or F5, near the point where deep convection and emission cores in Ca H and K make their first appearance. However, the falloff in rotation actually begins higher up the main sequence near spectral type F0, where there is a clear break in the slope of the specific angular momentum curve (Kraft 1970; Gray 1982*b*). Since the T Tauri stars destined to become late-type dwarfs are known to be relatively slow rotators (Vogel and Kuhi 1981; Hartmann *et al.* 1986), and since recent studies of low-mass stars in the Pleiades and α Per clusters suggest that pre–main-sequence stars may be spun up to very rapid rotation rates as they contract toward the main sequence (Stauffer *et al.* 1984), this bend in the angular momentum curve may arise only after the low-mass stars reach the main sequence.

The steepness of this decline in rotation down the main sequence is more obvious on a linear scale than on the logarithmic scale, which we have adopted here for convenience (in order to display the full range of velocities). Similarly, the sharp decline in $v \sin i$ toward the cooler subgiants, which Gray and Nagar (1985) found, is more clearly evident in a linear plot than on the compressed logarithmic scale of Figure 1.

In the lower panel of Figure 1 (or in a linear plot of the same data) there is little indication in our sample of giants for the sharp break in rotational velocities near G5 III that Gray (1982*a*) has reported finding. Rather, rapid rotation seems to terminate near G0 III and to fall off progressively toward later spectral types from that point onward, with no sign of a discontinuity at G5. This same trend was also noticed by Rutten and Pylyser (1988). Since Gray published few details of his analysis, it is difficult for us to speculate why we might not see his rotational discontinuity. In the first instance, Gray did not

TABLE 3

DWARFS AND SUBGIANTS

Star	HD	M_V	B-V	v sin i (km s^{-1})	l_{bol} [a] (10^{-7})	F/f [b] (10^{17})	τ_c (days)	N_R	R(C II) [c] (10^{-7})	R(C IV) [c] (10^{-7})
β Cas	432	1.56	0.34	70.0	30.7	0.429	0.54	3.13	6.03	15.1
β Hyi	2151	3.81	0.62	<3.0	20.5	0.330	10.2	>1.99	0.64	0.88
HR 244	5015	3.92	0.53	6.0	3.07	2.29	5.46	1.70	<3.91	<6.51
υ^2 Cas	5395	3.17	0.96	...	5.00	0.612	...	...	<0.08	...
ρ Psc	8723	3.28	0.39	61.0	1.77	5.93	1.15	0.86	13.8	24.6
ν Psc	10380	2.50	1.36	...	8.94	0.163	...	...	<0.22	<0.31
α Tri	11443	2.19	0.49	93.0	11.1	0.793	3.78	0.46	33.6	57.3
χ Eri	11937	2.52	0.85	...	10.8	0.343	...	...	1.67	2.22
HR 784	16673	3.74	0.52	6.0	1.27	6.01	5.00	1.14	5.67	4.49
θ Per	16895	3.69	0.49	8.8	5.85	1.30	3.78	1.90	2.24	2.24
τ^1 Eri	17206	3.76	0.48	22.0	4.21	2.02	3.42	0.72	7.60	12.8
ι Per	19373	3.69	0.60	3.5	6.48	0.907	9.10	2.15	0.97	1.85
δ Eri	23249	3.81	0.92	2.2	12.5	0.273	...	...	0.88	0.79[d]
τ^6 Eri	23754	3.08	0.42	6.0	5.14	1.90	1.72	6.64	3.70	4.47[d]
43 Per	24546	3.06	0.41	...	1.94	5.20	...	...	4.74	3.76[d]
39 Tau	25680	5.09	0.62	3.0	1.18	5.29	10.2	0.89	7.03	8.22
45 Tau	26462	3.25	0.36	6.0	1.27	8.78	0.74	13.2	16.5	35.4
ϵ Ret	27442	3.57	1.08	...	6.24	0.405	...	...	0.58	<1.41
α Cae	29875	2.35	0.34	52.0	4.12	2.84	0.54	3.10	12.7	32.5
58 Eri	30495	4.61	0.64	8.0	1.74	3.28	11.4	0.79	5.06	10.9
ζ Dor	33262	4.37	0.52	<1.0	3.40	2.09	5.00	>9.07	10.3	22.6
γ Lep A	38393	4.14	0.47	11.0	9.49	0.839	3.08	1.40	<0.61	<0.81
χ^1 Ori	39587	4.43	0.59	9.4	4.65	1.40	8.54	0.60	9.25	11.2
HR 2102	40409	3.06	1.05	...	4.96	0.599	...	...	<0.22	<0.22
ν^2 CMa	47205	2.77	1.06	2.7	9.62	0.302	...	...	<0.72	<1.25
ξ Gem	48737	2.06	0.43	70.0	11.4	0.853	1.95	0.80	13.0	14.8
HR 2740	55892	2.50	0.32	54.0	3.98	3.18	0.39	3.71	9.19	18.7
α CMi	61421	2.71	0.42	6.0	181.	0.049	1.72	8.38	3.20	4.75
χ Cnc	69897	4.27	0.47	<1.0	2.26	3.90	3.08	>13.7	3.54[d]	<0.84
32 Lyn	72291	3.77	0.36	20.0	0.79	18.0	0.74	2.78	14.1	30.5
π^1 UMa	72905	4.70	0.62	9.5	1.50	4.17	10.2	0.35	12.0	17.3
10 UMa	76943	3.16	0.44	26.0	6.57	1.44	2.20	1.18	7.91	10.8
τ^1 Hya	81997	3.89	0.46	28.0	3.74	2.37	2.76	0.65	7.57	11.9
24 UMa	82210	2.69	0.77	4.9	4.48	0.894	18.2	1.57	5.36	5.36
θ UMa	82328	2.33	0.46	6.4	14.0	0.587	2.76	6.05	1.08	1.22[d]
HR 3991	88215	2.55	0.36	148.0	1.87	5.78	0.74	0.76	12.3	20.9
40 Leo	89449	3.37	0.45	18.0	3.18	2.51	2.47	1.52	5.99	7.89
37 UMa	91480	2.94	0.34	87.0	2.11	5.67	0.54	1.12	11.8	9.95
ι Leo	99028	2.52	0.41	19.0	6.71	1.46	1.51	3.10	16.4	22.4
β Vir	102870	3.70	0.55	4.0	9.56	0.752	6.42	2.18	2.09	2.30
α Crv	105452	3.25	0.32	16.0	5.93	2.24	0.39	8.53	12.8	...
HR 4867	111456	3.91	0.46	36.0	1.19	6.93	2.76	0.52	14.3	13.4
78 UMa	113139	2.59	0.36	92.0	2.68	3.92	0.74	1.22	17.2	23.9
β Com	114710	4.73	0.57	4.3	5.28	1.32	7.45	1.66	3.41	3.60
69 Vir	116976	3.61	1.09	...	4.56	0.637	...	...	0.24[d]	<1.40
HR 5156	119288	3.88	0.42	18.0	0.87	11.2	1.72	1.53	4.56	5.89
τ Boo	120136	3.35	0.48	17.0	4.05	2.25	3.42	1.08	<1.16	<4.44
η Boo	121370	2.85	0.58	13.0	21.8	0.374	7.99	0.81	1.39	2.07
12 d Boo	123999	2.95	0.54	15.0	3.02	2.71	5.93	0.91	<1.46	<1.32
ι Vir	124850	2.25	0.52	17.0	6.28	1.07	5.00	1.47	8.28	12.3
18 Boo	125451	2.12	0.38	42.0	1.69	6.86	1.00	2.30	14.8	27.8

TABLE 3—*Continued*

Star	HD	M_V	B-V	v sin i (km s^{-1})	l_{bol} [a] (10^{-7})	F/f [b] (10^{17})	τ_c (days)	N_R	R(C II) [c] (10^{-7})	- R(C IV) [c] (10^{-7})
θ Boo	126660	3.34	0.50	32.0	6.13	1.43	4.17	0.49	11.6	16.5
σ Boo	128167	3.62	0.36	7.5	4.04	2.86	0.74	8.73	5.69	<9.16
μ Vir	129502	2.15	0.38	46.0	7.17	1.32	1.00	2.34	15.6	15.5
HR 5529	130817	2.77	0.36	20.0	0.85	13.2	0.74	4.94	...	<5.74
16 Lib	132052	2.49	0.32	117.0	4.01	3.15	0.39	1.72	8.55	13.4
χ Her	142373	3.37	0.57	2.2	3.66	1.92	7.45	2.28	1.09	<1.80
γ Ser	142860	3.47	0.48	8.0	7.72	0.902	3.42	2.55	<1.20	<0.92
14 Oph	150557	3.13	0.32	70.0	1.21	9.30	0.39	2.23	8.33	25.0[d]
ζ Her	150680	2.85	0.65	2.9	20.3	0.320	12.0	2.78	1.48	1.38
19 Dra	153597	3.84	0.48	9.0	2.88	2.73	3.42	1.77	6.39	...
47 Oph	157950	2.06	0.41	50.0	3.90	2.61	1.51	1.43	10.4	13.6
μ Her	161797	4.04	0.75	1.2	11.7	0.518	...	...	0.83	1.03
HR 6670	162917	3.67	0.42	25.0	1.25	7.85	1.72	1.22	8.68	12.9
73 Oph	166233	3.12	0.37	95.0	1.26	8.19	0.86	0.79	<6.31	5.31
η Ser	168723	2.08	0.94	2.6	16.3	0.228	...	...	0.35	0.46
χ Dra	170153	4.11	0.49	2.5	9.71	0.849	3.78	5.00	1.24[d]	<0.63
HR 6985	171802	2.70	0.37	14.0	1.75	6.74	0.86	6.15	15.5	19.9
110 Her	173667	2.77	0.46	14.0	5.33	1.83	2.76	2.05	6.19	10.5
59 Dra	180777	3.44	0.31	63.0	2.18	5.97	0.32	2.46	16.9	30.6
31 Aql	182572	3.90	0.77	2.3	2.55	1.80	...	...	<3.91	<2.77
θ Cyg	185395	3.22	0.38	5.3	3.99	2.80	1.00	11.2	7.25	13.3
β Aql	188512	3.14	0.86	2.6	10.5	0.405	...	...	0.78	<0.52
δ Pav	190248	4.79	0.76	...	11.2	0.430	17.8	...	0.89	1.70
HR 7925	197373	2.62	0.46	30.0	1.01	9.41	2.76	1.04	13.5	14.4
ψ Cap	197692	4.10	0.43	41.0	5.49	1.97	1.95	0.51	11.3	23.7
HR 7955	198084	2.82	0.54	5.0	4.15	1.79	5.93	3.05	2.41	<1.20
η Cep	198149	2.83	0.93	2.6	13.5	0.301	...	...	0.96[d]	<0.82
ϵ Equ	199766	1.84	0.46	54.0	2.07	6.29	2.76	0.71	13.7	19.6
ν Oct	205478	2.38	1.00	...	10.8	0.309	...	...	0.35	<0.43
μ^1 Cyg	206826	3.18	0.48	4.0	3.23	3.13	3.42	4.70	2.92	3.11
16 Cep	209369	2.62	0.44	27.0	2.49	3.82	2.20	1.46	18.7	34.0
ι Peg	210027	3.33	0.44	6.5	7.97	1.18	2.20	4.37	3.01	2.76[d]
ξ Peg	215648	2.77	0.50	8.9	5.45	1.56	4.17	2.31	0.79	1.32
7 And	219080	3.06	0.29	59.0	3.80	3.68	0.22	4.39	29.3	23.9
ψ^1 Aqr	219449	2.66	1.11	...	7.57	0.384	...	...	<1.00	...
υ Peg	220657	2.18	0.61	79.0	4.78	1.23	9.67	0.18	20.9	35.6
ι Psc	222368	3.51	0.51	5.7	5.79	1.42	4.58	2.39	<1.02	<3.45
γ Cep	222404	2.37	1.03	<1.0	17.8	0.179	...	...	0.79	1.33

[a] Apparent bolometric luminosity of star at Earth.
[b] Ratio of stellar surface flux to flux observed at Earth.
[c] Normalized emission-line flux (= ratio of observed flux to l_{bol}).
[d] Uncertain flux.

identify the rapidly rotating G giants for which he took velocities from the literature and unpublished sources, and in the second he selectively excluded upper limits on v sin i only for the early giants, which may have introduced a strong bias in the trend of rotation rate with $B-V$. Consequently, at this point we cannot reach any certain conclusions on this matter.

For stars within or close to the main-sequence band, Table 3 lists our estimate of the convective turnover time, τ_c (Gilman 1980). We have computed τ_c for main-sequence stars from the polynomial in $B-V$ color index given by Noyes *et al.* (1984). According to Gilliland's (1985*a*) evolutionary tracks, this expression yields τ_c values for subgiants that are overestimated by no more than a factor of 2 as long as the stars lie within 0.75 mag of the main sequence. Table 3 also lists the value of the Rossby number, $N_R = P_{rot}/\tau_c$. The rotation period P_{rot} is known for some of the solar-type stars from the detection of photometric variability or from the modulation of their Ca II H and K emission features (Baliunas *et al.* 1983). However, for the majority of stars, we have estimated P_{rot} indirectly from their v sin i, combined with an estimate of the stellar radius, which we

TABLE 4

GIANTS

Star	HD	B-V	v sin i (km s^{-1})	l_{bol} [a] (10^{-7})	F/f [b] (10^{17})	R(C II) [c] (10^{-7})	R(C IV) [c] (10^{-7})
HD 483	483	0.70	52.0	0.36	15.0	5.83	13.9[d]
α Cas	3712	1.17	4.9	46.1	0.065	0.20[d]	<0.13
β Cet	4128	1.01	3.0	51.9	0.067	0.98	0.98
ψ^3 Psc	6903	0.69	95.0	1.63	3.27	14.4	42.5
η Psc	9270	0.97	...	11.9	0.294	0.42	0.74
16 Per	17584	0.34	160.0	4.87	2.71	4.49	8.16[d]
o Tau	21120	0.89	...	11.7	0.338	<0.08	<0.17
γ Tau	27371	0.99	2.4	11.8	0.291	0.42	1.27
δ Tau	27697	0.99	2.5	10.6	0.322	<0.28	<0.28
ϵ Tau	28305	1.01	2.5	13.0	0.263	<0.23	<0.23
θ^1 Tau	28307	0.95	3.4	9.99	0.371	1.00	1.60
15 Ori	33276	0.32	55.0	2.85	4.31	<7.59	17.2[d]
α Aur Aa	34029	0.90	6.0	161.	0.030	1.70	2.70
α Aur Ab	34029	0.60	36.0	110.	0.059	24.0	37.0
β Lep	36079	0.82	5.1	22.5	0.189	<0.26	<0.17
HR 1889	36994	0.43	60.0	0.62	14.6	19.4	29.0
45 Aur	43905	0.43	20.0	1.80	5.17	10.0	12.2
δ Col	44762	0.88	...	9.19	0.443	0.10	<0.22
25 Mon	61064	0.44	30.0	2.23	4.02	12.3	19.5
o Gem	61110	0.40	92.0	2.63	3.56	11.9	18.1
β Gem	62509	1.00	2.5	119.	0.027	...	<0.18
o UMa	71369	0.85	2.6	14.7	0.261	1.07	<0.55
35 Cnc	72779	0.68	87.0	0.62	8.80	22.6	53.2
ι Cnc	74739	1.03	<20.0	8.46	0.378	0.58	0.84
27 Hya	80586	0.94	<20.0	3.98	0.935	<0.25	<0.75
μ Vel	93497	0.90	...	26.3	0.158	2.19	3.63
δ Crt	98430	1.12	...	14.7	0.180	<0.33	<0.60
HR 4529	102574	0.58	<10.0	0.85	8.302	1.88[d]	4.71[d]
18 Com	108722	0.43	93.0	1.63	5.78	23.9	47.9
β Crv	109379	0.88	3.8	26.0	0.184	0.27	0.23
31 Com	111812	0.67	85.0	2.83	1.94	28.9	78.6
ϵ Vir	113226	0.94	2.7	22.2	0.197	0.39	0.52
γ Hya	115659	0.92	...	18.7	0.267	0.45	1.21
θ Cen	123139	0.99	...	52.9	0.060	0.11	0.20
δ Boo	135722	0.95	...	13.5	0.251	0.21	0.61
η Dra	148387	0.91	2.2	23.7	0.202	0.21[d]	0.17
β Her	148856	0.94	3.4	23.7	0.184	0.50	0.67
η Her	150997	0.92	8.0	12.7	0.321	0.85	1.23
ϵ Sco	151680	1.15	...	49.6	0.050	0.28	0.58
20 Oph	151769	0.47	14.0	3.49	2.23	8.57	13.1
84 Her	161239	0.65	<10.0	1.54	4.27	0.93[d]	3.33
θ Her	163770	1.35	3.4	11.9	0.182	...	<0.38
ν Oph	163917	0.99	...	15.2	0.236	0.27	<0.20
δ Dra	180711	1.00	...	19.4	0.192	0.40	<0.16

TABLE 4—*Continued*

Star	HD	B-V	v sin i (km s^{-1})	l_{bol} [a] (10^{-7})	F/f [b] (10^{17})	R(C II) [c] (10^{-7})	R(C IV) [c] (10^{-7})
α Sge	185758	0.77	5.2	5.05	1.06	3.53	<3.14
ϵ Dra	188119	0.89	...	9.02	0.485	<0.22	<0.89
HR 7606	188650	0.75	10.0	1.38	3.53	3.71[d]	<7.14
ϵ Cyg	197989	1.03	3.0	34.9	0.097	0.37	0.20
HR 8191	203842	0.47	100.0	0.73	11.4	10.3	16.4
20 Peg	209166	0.34	<20.0	1.42	7.86	7.86	7.14
31 Cep	214470	0.39	100.0	2.25	4.32	4.55	7.73[d]
HR 8626	214714	0.86	10.0	1.15	3.43	4.75	4.42
μ Peg	216131	0.94	7.0	13.0	0.303	<0.15	<0.15
π Cep	218658	0.82	4.7	5.05	0.810	2.35	<4.71
HR 9024	223460	0.79	20.0	1.23	3.57	12.5	31.7
ω Psc	224617	0.42	38.0	6.30	1.61	14.1	17.5

[a] Apparent bolometric luminosity of star at Earth.
[b] Ratio of stellar surface flux to flux observed at Earth.
[c] Normalized emission-line flux (= ratio of observed flux to l_{bol}).
[d] Uncertain flux.

obtain from the angular diameter predicted by the Barnes-Evans relation (1976) and the stellar parallax. To compensate for sin i projection effects, we include a statistical correction of $\pi/4$. Our calculation is equivalent to the expression for N_R given by WBS.

III. THE ACTIVITY OF COOL SUBGIANTS

a) Evolutionary Trends

The change of activity with age is perhaps most clearly illustrated by a plot of the ultraviolet line fluxes in an H-R diagram, which we present here in Figures 2 and 3. In Figure 2 the height of each diamond-shaped symbol indicates the strength of the normalized C IV flux, $R(\text{C IV}) = f(\text{C IV})/l_{bol}$, while the width of each symbol is proportional to the rotation rate, v sin i. The solid diamonds denote stars for which we have only upper limits to the line flux, and the circles represent stars of unknown v sin i, in which case the diameter of the circle is drawn proportional to the strength of R(C IV). We have also constructed H-R diagrams using the C IV surface flux F(C IV) and the C IV luminosity L(C IV), instead of R(C IV), but these drawings appear similar to Figure 2 in every respect and hence will not be presented here. For the purpose of our discussion of evolutionary effects upon activity and rotation, Figure 2 also shows the zero-age main sequence and three of Iben's evolutionary tracks for 1.0, 1.25, and 1.5 $M_\odot$ stars (starting from the point of hydrogen shell burning), as transformed to the color-magnitude plane by Herbig and Wolff (1966). We present a similar H-R diagram for the C II λ1335 line in Figure 3. Figure 4 is a more conventional plot of the *IUE* flux as a function of $B-V$, which we provide to illustrate the narrow range of high activity levels among the early F dwarfs as compared with the much broader range in activity of the solar-type stars (WBS; Walter and Linsky 1986; Simon and Landsman 1987).

In Figures 2 and 3, the stars with masses $M \geq 1.25\ M_\odot$ have high rotation rates and strong UV emission when they are close to the main sequence. As these stars evolve to the right in the H-R diagram, their rotation rates decline. According to Gray and Nagar (1985), this spin-down occurs suddenly near G0 IV, which corresponds to $B-V = 0.6$. A similar discontinuity does seem to be present in our group of stars, although admittedly neither our sample nor theirs is very large. At the same point in the H-R diagram, the C IV and C II emission both appear to fall sharply with the drop in rotation. The time scale that we infer for this decay in activity is of the order of 50–100 Myr, but as far as we can tell the change does not coincide with any critical rotation rate or any critical value of the Rossby number. The decline in UV emission that we observe is in sharp disagreement with Gilliland's (1985*a*) prediction of a strong resurgence in the activity of low-mass stars after they leave the main sequence.

For 1 $M_\odot$ stars there is approximately an order of magnitude decline in the intensity of the UV emission during their main-sequence lifetimes (SHB). There seems to be no further major change once these stars leave the main sequence. At $R \approx 10^{-7}$, the normalized fluxes of the 1 $M_\odot$ subgiants are comparable to the flux observed for the quiet Sun. The observations therefore contradict Gilliland's (1985*a*) prediction, but, in addition, they suggest that once the strength of the dynamo is greatly weakened, any further decay is greatly impeded. Previously, the same hypothesis was put forth by Wilson (1966), Kraft (1967), and Gray (1982*b*) to explain the apparent ineffectiveness of the dynamo magnetic brake at slow rotation rates.

b) Dependence of Activity upon Rotational Velocity

For rotating convective stars, whose surface activity presumably arises from a deeply seated dynamo, a correlation between chromospheric emission and rotation is expected, although present-day theory cannot yet predict the exact form that relationship might take. To date a number of empirical rotation-activity laws, which involve various different combinations of stellar parameters, have been devised (Noyes *et al.*

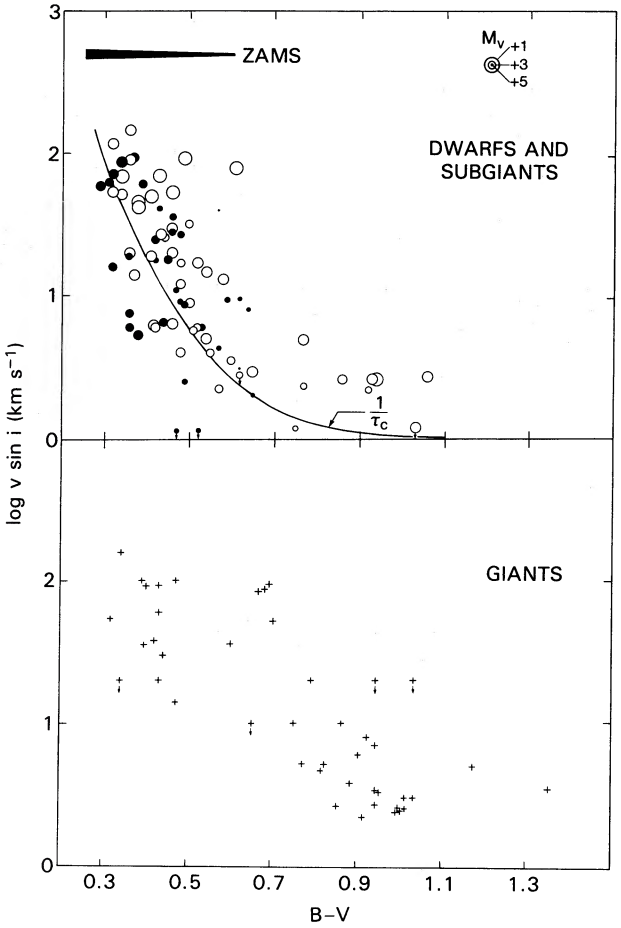

FIG. 1.—Projected rotational velocities for dwarf and subgiant stars (*upper panel*) and giant stars (*lower panel*) as a function of $B-V$ color. In the top panel, the size of each circle is proportional to the absolute visual magnitude of the star; the horizontal dark stripe depicts the variation of M_v along the ZAMS. Stars ≤ 0.5 mag or >0.5 mag above the ZAMS are represented by filled and open symbols, respectively. The solid curve is the reciprocal of the main-sequence convective turnover time (Noyes *et al.* 1984), normalized at the Sun. The decline in main-sequence rotation rates beginning at spectral type F0 is evident here. This decline is more obvious at the 75th percentile level than in the median (or mean) velocity, i.e., the falloff toward the cooler stars is most pronounced at the highest rotation speeds. The gradient is displayed more clearly on a linear scale than in the logarithmic plot used here. Similarly, the spin-down of the subgiants near G0 IV would also be more evident on the linear scale used by Gray and Nagar (1985). In the lower panel, the falloff in the rotation speeds of the giants starts near spectral type G0 III, and there is no sign of the discontinuity at G5 III that Gray (1982*a*) claims to exist.

1984; Mangeney and Praderie 1984; Vilhu 1984; SHB; Basri 1987; Simon and Fekel 1987).

Two such correlations are presented in Figure 5. This figure shows plots of the normalized flux in C IV and C II for the low-luminosity stars in our sample against their rotational velocities. For reasons to be explained in more detail below, we use symbols with different shading to distinguish between stars having $B-V<0.42$ and those having $B-V\geq 0.42$, i.e., between stars with spectral types earlier or later than F5. It is immediately obvious from Figure 5 that the later type stars obey a strong correlation between activity and rotation. Several stars deviate widely from the general trend. One of the most discrepant is ζ Dor, which has no measurable rotation at all according to *The Bright Star Catalogue*, but whose v sin i is estimated to be ~ 10 km s^{-1} by Danks and Lambert (1985) and 17 ± 2 km s^{-1} by Soderblom, Pendleton, and Pallavicini (1989). If we adopt the v sin i of Soderblom *et al.*, then virtually all of the apparent discrepancy for ζ Dor is eliminated. For the slowly rotating stars, whose location is the lower left-hand corner of each panel of Figure 5, the increased scatter is most likely due to observational uncertainties in the weak UV fluxes of these stars, as well as to systematic errors in their velocities, which dominate any random errors at these small rotation rates.

We have carried out least-squares regression analyses for the stars plotted in Figure 5. In our calculations we have included only those stars for which a chromospheric flux has been detected and a rotation rate has been measured, that is, we have ignored the relatively few stars with upper limits in either quantity. Our results should not be invalidated by the neglect of these upper limits because only a few stars were omitted. First, considering the stars with $B-V\geq 0.42$, we derive a log-linear (power-law) least-squares fit for C IV, viz.,

$$\log R(\text{C IV}) = -7.15 + 0.88 \log v \sin i\,,$$
$$\pm 0.28 \qquad \pm 0.12 \pm 0.10$$

for which the standard deviation is $\sigma_{\text{FIT}} = 0.28$ and the linear correlation coefficient is 0.83. Similarly, for C II we obtain the fit

$$\log R(\text{C II}) = -7.20 + 0.82 \log v \sin i\,,$$
$$\pm 0.27 \qquad \pm 0.09 \pm 0.08$$

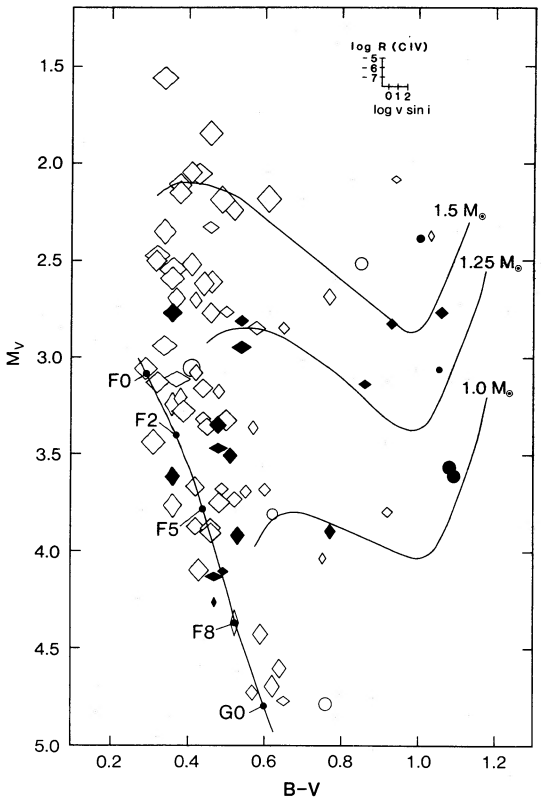

FIG. 2.—Color-magnitude diagram showing evolutionary effects on rotation and C IV transition region emission. The height of each diamond-shaped symbol is proportional to the strength of the normalized C IV flux, R(C IV), and the width is proportional to the rotation speed, v sin i. The scales are shown in the inset located in the upper right-hand corner of the figure. The solid symbols represent upper limits on the C IV flux. The circles denote stars for which v sin i is unknown; the diameters of the circles are proportional to R(C IV).

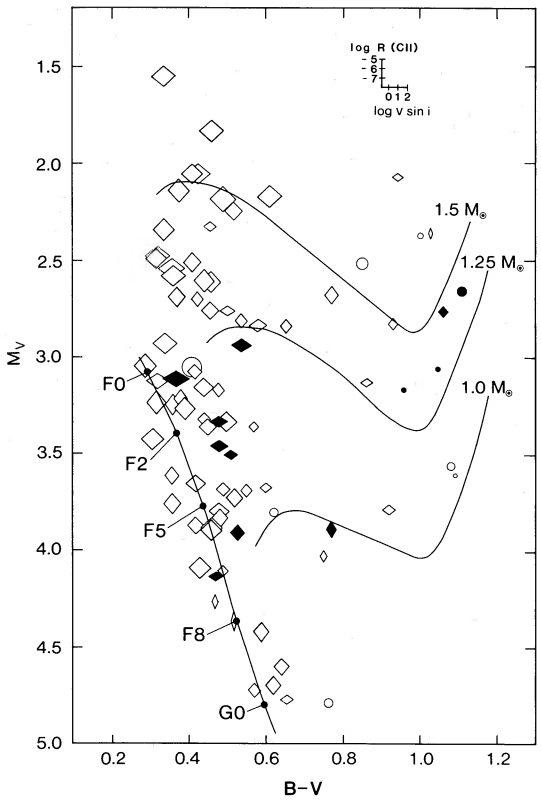

FIG. 3.—Same as Fig. 2, for the C II emission line

which also has a very large correlation coefficient of 0.83. Thus, the brightness of the UV lines is almost linearly proportional to the rotation rate, just as Skumanich (1972) found for the emission reversals in the Ca II H and K lines.

As is well known, the usual least squares method, which we used in the preceding calculations, assumes that the observational errors are exclusively in the ordinate (in our particular case, in the normalized flux) and that the abscissa (here the rotational velocity) is error-free. Since there are observational uncertainties in both variables, the normalized flux and the rotation rate, in this paper we have developed a double regression procedure to eliminate this restriction. The principal assumption of our double regression method (which is described more fully in the Appendix) is that the ratio of the errors in the ordinate and the abscissa, $\epsilon_{\log R}/\epsilon_{\log v \sin i}$, is identical from one star to the next. For our application as well as for many other common uses, this limitation is a relatively minor one.

Applying the double regression method to the previous least-squares calculation (for $B-V \geq 0.42$), we obtain the following fit to the normalized C IV flux:

$$\log R(\text{C IV}) = -7.41 + 1.12 \log v \sin i\,,$$
$$\pm 0.31 \qquad \pm 0.08 \pm 0.07$$

which has a standard deviation $\sigma_{\text{FIT}} = 0.31$. We find an equally tight fit for the C II emission,

$$\log R(\text{C II}) = -7.41 + 1.02 \log v \sin i\,.$$
$$\pm 0.29 \qquad \pm 0.07 \pm 0.06$$

To within the formal uncertainties of our calculations, there is no distinction between stars on the main sequence and those which are only slightly evolved, i.e., those which are within 0.5 mag of the ZAMS and which have not crossed over to the base of the red giant branch. Therefore, both groups of stars are combined to arrive at the foregoing regression solutions.

We have carried out similar regression calculations for the warmer stars at $B-V < 0.42$ (those represented by the open symbols in Fig. 5). It was originally shown by Walter (1983) for X-ray emission, and subsequently by WBS for UV emission, that the intense activity of these stars is uncorrelated with stellar rotation. Since the sample of stars analyzed here is larger than the one available to WBS, we have reexamined this issue. Our least-squares solution for the normalized flux in C IV yields the formal result

$$\log R(\text{C IV}) = -5.38 - 0.20 \log v \sin i\,,$$
$$\pm 0.20 \qquad \pm 0.18 \pm 0.11$$

which has a linear correlation coefficient of -0.26, and for C II we find

$$\log R(\text{C II}) = -6.02 + 0.06 \log v \sin i\,,$$
$$\pm 0.17 \qquad \pm 0.13 \pm 0.08$$

with a linear correlation coefficient of 0.12. We regard the slopes of these relations as indistinguishable from zero and

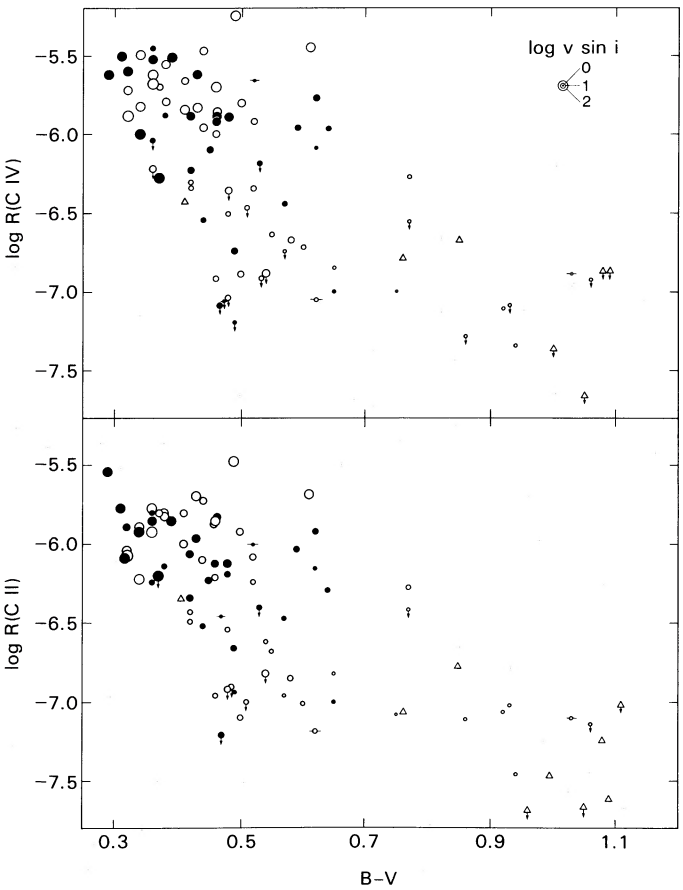

FIG. 4.—Normalized UV line flux of dwarfs and subgiants plotted against $B-V$ color for C IV (*upper panel*) and C II (*lower panel*). Filled and open symbols represent stars closer than or farther than 0.5 mag above the ZAMS, respectively. The size of each circle is proportional to v sin i. Upper limits on v sin i are indicated by the horizontal sidebars, and stars whose rotation rates are unknown are shown as small triangles.

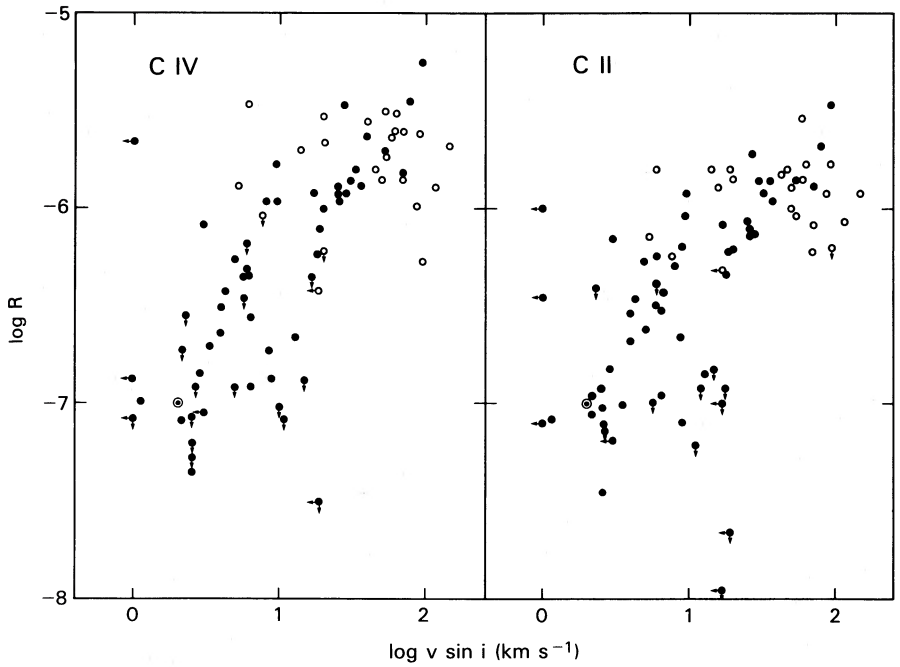

FIG. 5.—Plots of normalized C IV flux (*left-hand panel*) and C II flux (*right-hand panel*) against v sin i for dwarfs and subgiants. The solid circles denote stars with $B-V \geq 0.42$, the open circles those with $B-V < 0.42$. The circled dot represents the Sun.

conclude that the emission of the early F stars is independent of rotation rate. If we include nine additional stars[4] with $B-V < 0.42$ from Simon and Landsman (1987), then the regression for C IV becomes

$$\log R(\text{C IV}) = -5.52 - 0.08 \log v \sin i\,,$$
$$\pm 0.20 \qquad \pm 0.09 \pm 0.06$$

which is identical to the result cited above, to within the errors.

Although the range in v sin i of the early F stars covers more than a decade, this range is still less than that of the stars with $B-V \geq 0.42$, since the latter group includes some very slow rotators. To show that this narrower range of velocity is *not* the reason why the activity of the hotter stars appears uncorrelated with rotation, we have repeated the least-squares regression for the cooler stars but restricted the velocity range to v sin $i \geq 6$ km s^{-1}, the same as for the hotter stars. This yields a regression for C IV

$$\log R(\text{C IV}) = -7.74 + 1.34 \log v \sin i\,,$$
$$\pm 0.32 \qquad \pm 0.18 \pm 0.14$$

which is still significant according to the standard errors of the fit and the linear correlation coefficient of 0.76. Considering the strength of this correlation, we conclude that the smaller velocity range of the early F-type stars is not the reason why their activity and rotation appear uncorrelated, although the addition of more slowly rotating stars to this sample (if others can be found) would certainly help to confirm this result.

To emphasize just how sharp this dichotomy in the relationship between activity and rotation appears to be, we have binned our sample of stars into narrow intervals of $B-V$ color and repeated the least-squares calculations separately for each group. For stars in the range $0.38 \leq B-V \leq 0.41$, we find no convincing correlation between C IV (or C II) emission and v sin i; yet stars in the color interval $0.42 \leq B-V \leq 0.45$ follow virtually the same correlation we derived earlier for the entire sample of stars with $B-V \geq 0.42$.

In a parallel study, Walter and Schrijver (1987) have claimed that the UV emission of the early F stars consists of two components, a "basal" or rotation-independent component that accounts for *most* of the flux observed for individual stars, and a second, weaker component that scales with the rotation rate. According to those authors, if a color-dependent basal flux is subtracted from the observed flux, then the residual component is strongly correlated with v sin i. We have attempted a similar analysis here for our larger sample of stars, using both the normalized line flux and the surface flux. We find that when we remove a basal flux of varying size from the C IV emission of the early F stars, there is no statistically significant correlation present between the residual flux and the stellar rotation rate. As measured by the linear correlation coefficient or by the standard error of the fit, the best correlation between the C IV flux and v sin i is found when there is *no* such basal term at all. It is unclear to us why our results contradict those of Walter and Schrijver. However, as we will discuss in § IIIc, we believe that the Rossby numbers of the early F stars, in general, are so large ($N_R \gg 1$) that any rotation-dependent component to the observed flux should be tiny, certainly much smaller than what was inferred by Walter and Schrijver.

To explain the differences that exist between the rotation-activity relations for stars earlier than F5 and those later than F5, one might suppose that for some as yet unknown reason the correlation found for the cooler stars is the result of viewing those stars (but not the earlier ones) at different orientations of their rotation axes. The most intense activity of the Sun is confined to latitudes close to the solar equator and avoids regions near the poles (Howard and LaBonte 1981), so it is entirely plausible that the activity of other stars might be concentrated at equatorial latitudes, too. Then, one might

[4] This group includes 22 Boo, 83 Tau, 8 Dra, 53 Her, η Lep, HR 7887, β Cae, 48 Tau, and η Sco. Most were omitted here for lack of a reliable parallax.

expect that stars viewed nearly pole-on would have both a low v sin i and weak chromospheric emission, while those observed close to equator-on would exhibit both rapid rotation and strong emission. However, it has been demonstrated elsewhere that chromospheric activity is strongly correlated with rotation periods (Noyes *et al.* 1984; SHB; § IIIc of this paper), which are independent of an observer's viewing angle, and so we believe that any such proposal is unsupportable.

We can suggest another possible explanation, namely, that the early F stars have at most a weak gradient of activity from equator to pole and all have approximately the same equatorial velocity but are viewed at different inclination angles. Since rotation periods are known for very few of our stars, we cannot exclude the possibility of such a coincidence in a group of fewer than two dozen stars, however unlikely that explanation might be for a large sample of stars. Following the treatment outlined by Kraft (1965) and Gray (1982*b*), we find that the frequency distribution of v sin i values for the stars with $B-V < 0.42$ is reasonably consistent with a Maxwell-Boltzmann distribution of v_{eq} and a random orientation of rotation axes but is much too broad for a single high value of v_{eq} and a random distribution of inclinations. Thus, in our sample, 43% of the stars fall within the limits of 0.6 and 1.3 times the average v sin i, and 83% lie within the limits of 0.2 and 1.8 times the mean, while the values expected for a Maxwell-Boltzmann law are 50% and 90%, respectively.

c) *Dependence of Activity upon the Rossby Number*

An examination of the individual points plotted in Figure 5 for the stars with $B-V \geq 0.42$ shows that the amount by which they deviate from the C IV and C II regression lines depends on the $B-V$ color. A similar color dependence was noted for the Ca II H and K emission by Noyes *et al.* (1984), who removed this effect by introducing the Rossby parameter, $N_R = P_{rot}/\tau_c$, as a measure of the rotation rate.

Using the values of N_R from Table 3, we have replotted the normalized C IV and C II fluxes against this parameter in Figure 6, and for comparison we have also plotted the Rossby relations for solar-type stars derived by SHB. At very large Rossby numbers, these curves may asymptotically approach a constant basal flux level (Schrijver 1987), but we are not aware of any observations of transition region lines that have actually detected such basal fluxes. The stars in our sample with $B-V \geq 0.42$ and of known rotation period adhere closely to the Rossby relations, but among those for which only v sin i is known there are some very discrepant points. Some of this increased scatter may be due to sin i projection effects. We have tried to illustrate this effect by means of the dashed lines, which are displaced from the Rossby curves by a factor of 2. The two most discrepant stars are ζ Dor, whose v sin i is probably underestimated (as we noted earlier), and χ Cnc, which has only an upper limit on v sin i. For the stars later than F5, the standard deviation of the scatter around the C IV and C II Rossby relations is $\sigma_{\log R} = 0.5$, which is comparable to the standard deviation that we derived for the log-linear fits of the normalized fluxes to v sin i in § III*b*.

For the early F stars with $B-V < 0.42$, we see that the C IV and C II emission is uniformly high and independent of N_R. This pattern was first noted by WBS in a smaller sample of stars. Moreover, according to calculations performed by Rucinski and VandenBerg (1986), the τ_c values of Noyes *et al.* (1984) that we have used here for the early F stars may be systematically too large, and so their N_R may be underestimated. Therefore, in Figure 6 we may need to shift these points even farther from the Rossby curves. Given these large values of N_R, if the early F stars indeed have an emission component that depends on N_R and follows the same Rossby relation that applies to stars later than F5, then this component must be a very small portion of the total flux observed.

The more highly evolved subgiants have been excluded from Figure 6, either because their v sin i is unknown or because it is hard to estimate the value of τ_c for these stars to better than an order of magnitude from the limited calculations published to date (Gilliland 1985*a*). In the first place, Gilliland presented

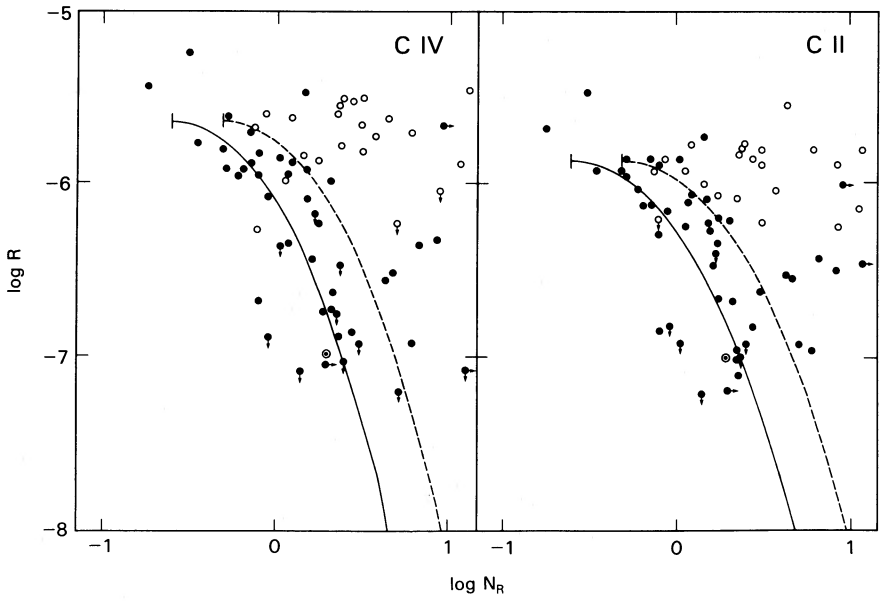

FIG. 6.—Plots of normalized C IV flux (*left-hand panel*) and C II flux (*right-hand panel*) versus the Rossby number N_R for stars within 0.75 mag of the ZAMS. Symbols have same meaning as in Fig. 5. The solid line is the Rossby relation for solar-type stars from SHB, while the dashed line is the same relation offset by a factor of 2 in N_R to illustrate the effects of a scatter in inclination angles on the values of N_R.

evolutionary tracks and detailed results on τ_c only for 1 and 1.58 $M_\odot$, and in the second place, his theoretical tracks are difficult to reconcile with the observationally determined position of the giant branch in the color-magnitude diagram. Notwithstanding these problems, Gilliland's calculations do predict relatively long convective turnover times of order 100 days for the coolest subgiants, e.g., η Cep and β Aql. For a reasonable equatorial velocity estimate of $v_{eq} \approx 2.5$ km s^{-1}, the Rossby numbers for these stars turn out to be of order unity, $N_R \approx 1$. If the evolved subgiants follow the same Rossby relation as do the dwarfs, then they should have relatively weak chromospheric emission, and so it is not surprising that we find no trace of the resurgence in activity which Gilliland predicted for evolved stars.

d) X-Ray Emission and Acoustic Heating

Although many late-type stars have now been observed at far-UV wavelengths, many fewer of them have been observed at X-ray wavelengths. Consequently, there is much less information available on coronal plasmas at temperatures above 10^6 K than there is on chromospheric and transition region plasmas at temperatures below 250,000 K. The X-ray fluxes that we have gathered from the literature or have assembled both from our own unpublished *Einstein* observations and from other images released from the *Einstein* archives, are listed in Table 5. This compilation should be nearly complete for the early F stars and for the late-type subgiants in our UV sample, but it includes only enough data for the cooler dwarf stars to provide an adequate comparison with the hotter stars. These X-ray fluxes are plotted in an H-R diagram in Figure 7 and are shown as a function of $B-V$ in Figure 8.

The X-ray observations are obviously much too incomplete to reveal any evolutionary trends as clear as those that were apparent in the UV H-R diagrams. All the same, these data prove to be valuable in other ways, as we will now show.

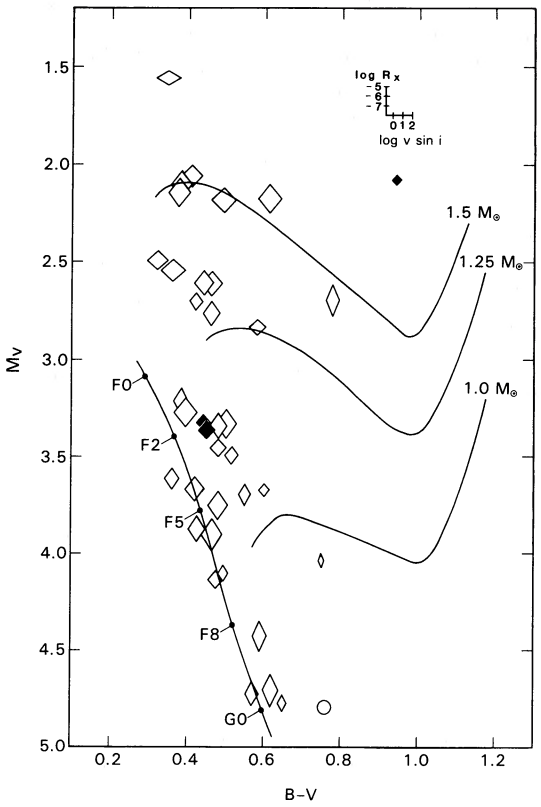

FIG. 7.—An H-R diagram for X-ray emission. Symbols have the same meaning as in Figs. 2 and 3.

Walter (1983) was the first to notice that X-ray emission is correlated with rotation speed for dwarf stars with $B-V \geq 0.45$ but not for those at smaller $B-V$. He surmised that there might be a demarcation line at $B-V = 0.45$

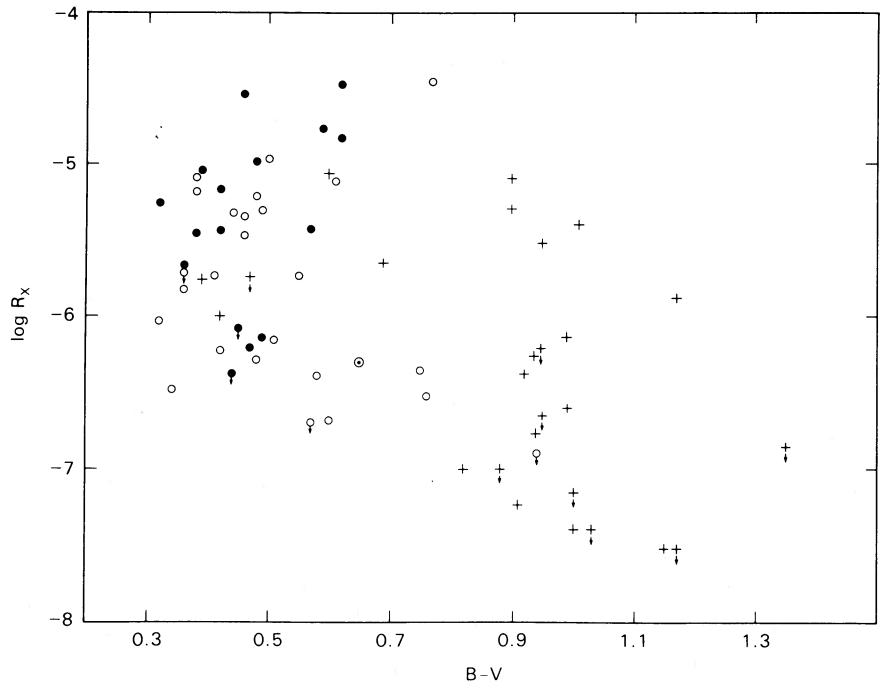

FIG. 8.—Plot of normalized X-ray emission as a function of $B-V$ color. The filled circles denote dwarfs and subgiants within 0.5 mag of the ZAMS. The open circles are subgiants lying more than 0.5 mag above the ZAMS. The plus symbols represent luminous giants.

TABLE 5

RESIDUALS IN X-RAY EMISSION[a]

Star	B - V	log R(C IV) (Observed)	log R_X (Observed)	Δ log R_X(O-C)
		a) Dwarfs and Subgiants		
HR 2740	0.32	-5.721	-6.041	-1.648
α Crv	0.32	...	-5.261	...
β Cas	0.34	-5.824	-6.479	-1.935
HR 3991	0.36	-5.678	-5.824	-1.493
σ Boo	0.36	<-6.036	-5.678	>-0.817
HR 5529	0.36	<-6.244	<-5.724	...
18 Boo	0.37	-5.553	-5.182	-1.030
μ Vir	0.38	-5.796	-5.079	-0.577
θ Cyg	0.38	-5.886	-5.462	-0.827
ρ Psc	0.39	-5.602	-5.040	-0.818
47 Oph	0.41	-5.854	-5.747	-1.160
α CMi	0.42	-6.319	-6.228	-0.929
HR 5156	0.42	-6.229	-5.176	-0.018
HR 6670	0.42	-5.886	-5.447	-0.812
16 Cep	0.44	-5.469	-5.325	-1.291
ι Peg	0.44	-6.553	<-6.383	<-0.707
40 Leo	0.45	-6.102	<-6.086	<-1.124
HR 4867	0.46	-5.886	-4.545	0.090
110 Her	0.46	-6.000	-5.474	-0.668
HR 7925	0.46	-5.854	-5.356	-0.768
γ Lep	0.47	<-7.092	-6.221	>0.367
τ^1 Eri	0.48	-5.886	-4.987	-0.352
τ Boo	0.48	<-6.357	-5.218	>0.141
γ Ser	0.48	<-7.036	-6.297	>0.195
α Tri	0.49	-5.244	-5.312	-1.584
χ Dra	0.49	<-7.201	-6.148	>0.633
θ Boo	0.50	-5.796	-4.967	-0.464
ι Psc	0.51	<-6.469	-6.161	<-0.622
β Vir	0.55	-6.638	-5.745	0.071
β Com	0.57	-6.444	-5.431	0.068
η Boo	0.58	-6.678	-6.399	-0.517
χ^1 Ori	0.59	-5.959	-4.777	-0.034
ι Per	0.60	-6.721	-6.697	-0.743
39 Tau	0.60	-6.086	-4.827	0.110
υ Peg	0.61	-5.444	-5.122	-1.122
π^1 UMa	0.62	-5.770	-4.478	-0.014
Quiet Sun	0.65	-7.000	-6.301	0.128
μ Her	0.75	-7.000	-6.361	0.068
δ Pav	0.76	-6.770	-6.530	-0.495
24 UMa	0.77	-6.268	-4.458	0.760
η Ser	0.94	-7.337	<-6.903	<0.122

between dynamo-generated activity in the cooler stars and activity induced by primordial magnetic fields in the hotter stars. We have repeated Walter's regression analysis here, except that we have divided our X-ray sample into two groups at $B-V = 0.42$ to be consistent with the UV results we presented earlier.

For the cooler stars we broadly confirm Walter's results, although the exact numerical values we derive depend on whether or not we include the young, active solar-type stars; our correlation coefficients also tend to be somewhat lower than his. The strong likelihood of such a correlation is suggested by the left-hand panel of Figure 9, which also illustrates the large scatter in these X-ray data. The right-hand panel of Figure 9 is a plot of the normalized X-ray flux versus N_R and a

TABLE 5—*Continued*

Star	B - V	log R(C IV) (Observed)	log R_X (Observed)	Δ log R_X(O-C)
		b) Giants		
α Cha	0.39	...	-5.767	...
ω Psc	0.42	-5.757	-6.013	-1.568
HR 8191	0.47	-5.785	<-5.745	<-1.258
α Aur Ab	0.60	-5.432	-5.013[b]	-1.030
ψ^3 Psc	0.69	-5.372	-5.658	-1.757
β Lep	0.82	<-7.759	-7.000	>0.808
β Crv	0.88	-7.636	<-7.000	<0.576
α Aur Aa	0.90	-6.569	-5.260[b]	0.442
μ Vel	0.90	-6.440	-5.097	0.396
η Dra	0.91	-7.777	-7.237	0.605
γ Hya	0.92	-6.921	-6.376	-0.084
ϵ Vir	0.94	-7.282	-6.770	0.157
β Her	0.94	-7.176	-6.260	0.477
μ Peg	0.94	<-7.812	<-6.211	...
θ^1 Tau	0.95	-6.796	-5.523	0.557
δ Boo	0.95	-7.217	<-6.670	<0.140
γ Tau	0.99	-6.896	-6.143	0.107
δ Tau	0.99	<-7.553	-6.599	>0.822
β Gem	1.00	<-7.733	-7.395	>0.363
δ Dra	1.00	<-7.801	<-7.167	...
β Cet	1.01	-7.008	-5.402	1.041
ϵ Cyg	1.03	-7.706	<-7.398	<0.308
ϵ Sco	1.15	-7.237	-7.523	-0.678
α Cas	1.17	<-7.886	<-7.517	...
37 Com	1.17	...	-5.870	...
θ Her	1.35	<-7.417	<-6.854	...

a Excess or deficit of X-ray flux based on observed C IV flux and Rossby relation for dwarf stars.
[b] Observed X-ray flux of Capella divided equally between components Aa and Ab (Ayres *et al.* 1983).

comparison with the Rossby relation of SHB for stars of known P_{rot}. Given the small size of our sample, we consider the overall agreement with the Rossby relation to be highly satisfactory. We also confirm Walter's finding that the X-ray emission of the early F stars is uncorrelated with $v \sin i$, except for some small differences with the numerical values in his Table 2. This result is consistent with the appearance of Figure 9 but is perhaps not entirely convincing for such a small group of stars.

It is more important that the X-ray fluxes of the early F stars are fainter than those of the most active solar-type stars, whereas the UV lines of these two groups were previously shown to be of equal brightness. This distinction between the X-ray and UV brightness of the early F stars is most clearly demonstrated by flux-flux plots such as those presented in Figure 10. In the left-hand panel, which displays the C IV–C II correlation, the early F stars lie at the high-activity end of the mean relation for solar-type stars; their line flux ratios therefore appear solarlike, although these stars lie higher up the curve than is appropriate for their Rossby numbers. Consequently, at temperatures below 250,000 K the differential emission measure curves of these stars should have the same shape as those of solar-type stars (e.g., Jordan *et al.* 1987),[5] but may be shifted in scale.

On the other hand, in the X-ray versus C IV diagram presented in the right-hand panel of Figure 10, the early F stars

[5] Ayres, Marstad, and Linsky (1981) and Oranje (1986) reported that the early F stars deviate systematically from the cooler stars in their flux-flux diagrams, which plot various chromospheric, transition region, and coronal diagnostics against the chromospheric Mg II flux. We have remeasured the F star spectra used by those authors and have determined that their Mg II line strengths were underestimated by factors of 2–10. With our larger fluxes the F stars no longer appear anomalous.

To date, none of the early F stars has been subjected to a differential emission measure analysis. The earliest star to be analyzed is the F5 IV–V star α CMi (Procyon), for which Jordan *et al.* (1986) derived a very nonsolarlike emission measure distribution. The X-ray flux and luminosity cited by those authors are an order of magnitude smaller than the values given by Schmitt *et al.* (1985*b*), although both groups apparently arrived at the same coronal emission measure (log EM = 50.6). The flux cited by Jordan *et al.* refers to the 0.5–4.5 keV energy band, whereas that of Schmitt *et al.* refers to the 0.15–4.0 keV band. The bandpass of Schmitt *et al.* covers more of the low-energy channels of the IPC and is the more appropriate one to use for a soft X-ray source like Procyon, $T_{cor} \approx 10^{6.2}$ K, since it includes a larger portion of the total X-ray luminosity. The Schmitt *et al.* flux is the one we adopt here.

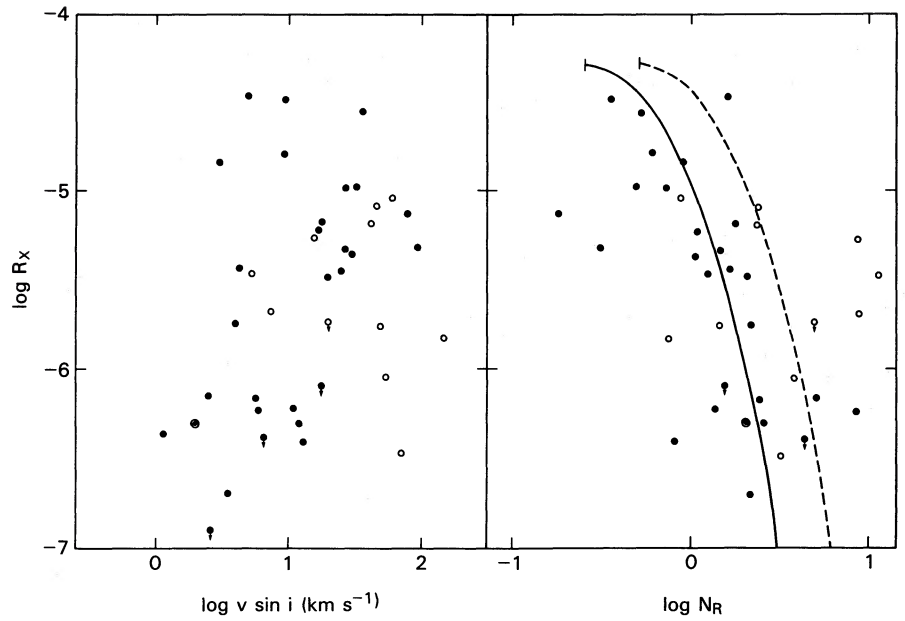

FIG. 9.—Plots of normalized X-ray emission against rotational velocity $v \sin i$ (*left-hand panel*) and Rossby number N_R (*right-hand panel*) for dwarfs and subgiants. Stars with $B-V \geq 0.42$ are shown as solid circles, those with $B-V < 0.42$ as open circles. The solid line is the Rossby relation for solar-type dwarfs from SHB, and the dashed line is the same relation displaced by a factor of 2 in N_R.

fall systematically below the Rossby relation defined by the solar-type stars. That is, for a given UV flux, the early F stars produce substantially less X-ray emission than do the solar-type stars. Some cooler stars with $B-V \geq 0.42$ also lie in the same region beneath the curve, but nearly all of these points correspond to high-luminosity stars with $M \geq 1.25\ M_\odot$ or to lower luminosity stars with $B-V$ colors within a few hundredths of a magnitude of $B-V \approx 0.42$. For example, the F5 IV–V star Procyon lies below the curve, but its position in the H-R diagram between the 1.25 and 1.5 $M_\odot$ evolutionary tracks (cf. Fig. 7) belies its larger, astrometrically well-established mass of 1.76 $M_\odot$ (van de Kamp 1954; Demarque and Guenther 1986). The only stars at $B-V > 0.46$ that fall far from the curve are ι Per, for which the published X-ray fluxes disagree by a factor of ~ 3 (the lower, more discrepant value is adopted here), and 24 UMa, which is much brighter in X-rays than expected for its C IV flux. Since the X-ray and UV observations were not made simultaneously, it is not surprising that there is more scatter in this plot than in the C IV–C II plot.

Now, for each point plotted in the right-hand panel of Figure 10 we have measured the vertical distance to the Rossby curve, which serves as a measure of that star's X-ray deficit or excess. Note that this deviation is measured with respect to the X-ray flux expected for a solar-type star of the same C IV strength. We have also computed the deviations from an X-ray–C II diagram and obtained essentially the same results,

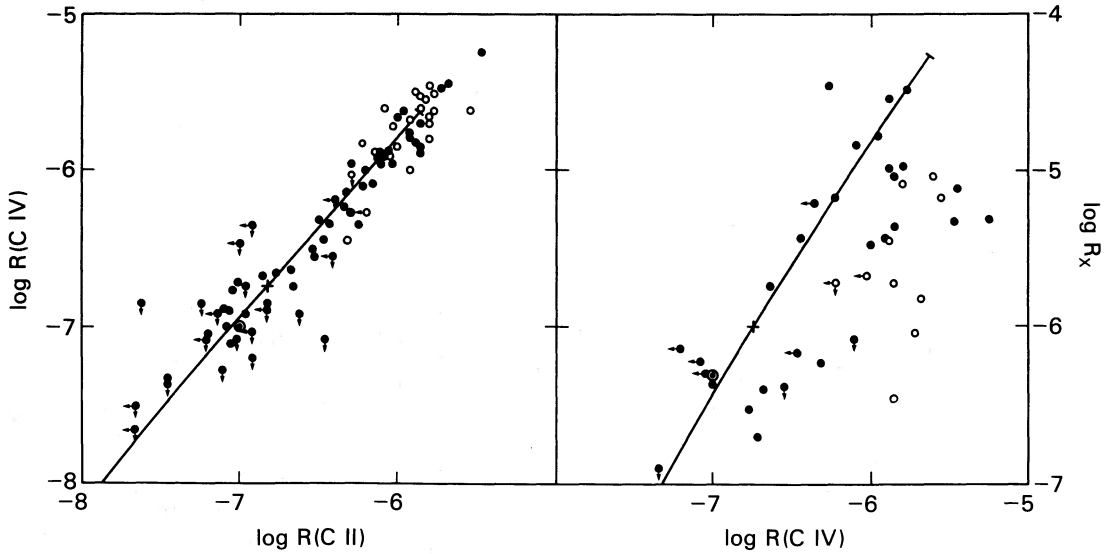

FIG. 10.—Flux-flux plots for dwarfs amd subgiants. The solid and open circles denote stars with $B-V \geq 0.42$ and $B-V < 0.42$, respectively. In both panels, the solid line is the Rossby relation from SHB. The plus sign along each relation denotes the position of the quiet Sun according to the solar N_R, while the position of the Sun as actually observed is shown by a circled dot.

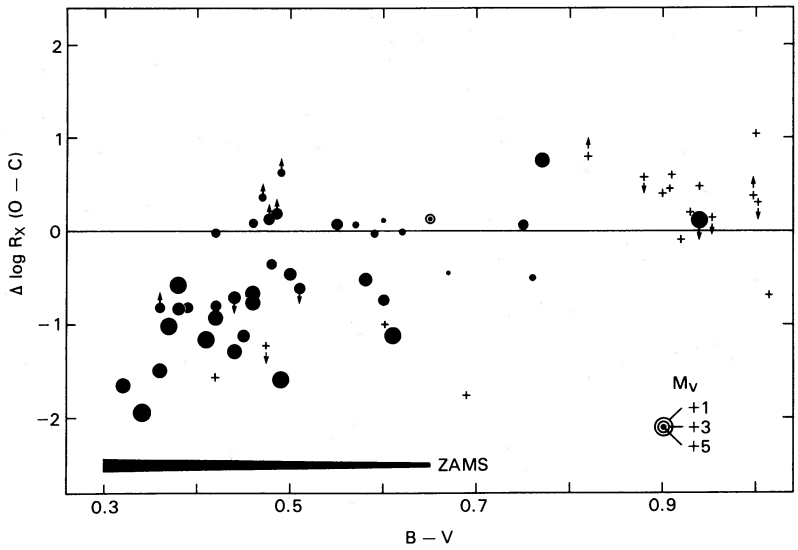

FIG. 11.—Residuals in X-ray emission plotted as a function of $B-V$ color for dwarfs and subgiants (*circles*) and for giants (*plus signs*). The size of each circle is proportional to the absolute visual magnitude M_v. The variation of M_v along the ZAMS is depicted by the horizontal bar at the bottom of the figure. A deficit (surplus) in R_X corresponds to the vertical distance below (above) the flux-flux relation at which each point lies in the preceding figure (in the sense *observed* minus *expected* based on the observed C IV flux).

since, as the left-hand panel of Figure 10 shows, the UV fluxes closely scale with one another. As far as we can determine, the deviation in X-ray emission is correlated solely with $B-V$ color and luminosity but with no other stellar parameters. For example, we can find no obvious dependence on rotation rate.

These deviations in X-ray emission are plotted in Figure 11 as a function of $B-V$ color and with their symbols keyed to the absolute visual magnitude M_v. The largest X-ray deficiencies are associated with the earliest stars and with the most luminous stars. The deficiencies vanish at $B-V \approx 0.42$ for the main-sequence stars, but persist to cooler $B-V$ for the more luminous, evolved stars. All that remains at $B-V \geq 0.42$ for the dwarf stars is a scatter of a factor of 2–3, which we are inclined to identify with ordinary time variability in coronal structure.

Since the detection of chromospheric and transition region lines with *IUE* becomes progressively more difficult for stars of early spectral type, we have restricted our sample to those having $B-V > 0.28$. The detection of transition region emission in the C IV line from low-dispersion *IUE* spectra is especially problematical for the A stars because of the complex appearance of their photospheric absorption-line spectra (Simon and Landsman 1987). On the other hand, Schmitt *et al.* (1985*a*) have detected weak X-ray emission from several apparently single A-type stars, including α Aql ($B-V = 0.22$) and α Hyi ($B-V = 0.28$). There is no firm evidence in *IUE* spectra of α Aql for emission at either C II or C IV (the evidence for emission at Lyman-α is conclusive), but these lines are definitely present in *IUE* spectra of α Hyi (Simon and Landsman 1987). The emission-line fluxes measured for α Hyi are consistent with an X-ray flux deficit of ~2 orders of magnitude, i.e., Δ log $R_X \approx -2$. Therefore, it is quite likely that the systematic weakening of X-ray emission found among the early F stars continues upward into the more massive A-type stars.

A possible explanation for this trend, which we would like to discount, is that the X-ray deficiencies of the early F stars are simply an instrumental artifact. Schmitt *et al.* (1985*a*) were careful to point out that the X-ray spectra observed by the imaging proportional counter (IPC) of the *Einstein Observatory* for the A and early F stars, in particular those of α Aql and α Hyi, appear to be much softer than those of the G and K stars. That is, the coronae of the early-type stars tend to be distinctly cooler than those of the solar-type stars. In order to include the soft energy channels of the IPC, and hence a larger fraction of the X-ray luminosity of A–F stars, Schmitt *et al.* used a bandpass of 0.15–4.0 keV. They also adjusted the IPC flux calibration for these low-energy X-ray photons. Maggio *et al.* (1987) adopted the same 0.15–4.0 keV energy band for measuring the X-ray fluxes of a sample of late F and G dwarfs, but chose a different flux calibration factor to account for the harder X-ray spectrum. We also used the identical bandpass in our own IPC measurements. Thus, the three sets of data from which the large majority of X-ray fluxes in this paper have been taken were all measured in a consistent way.

Based upon calculations for a thermal spectrum (continuum plus lines, assuming solar abundances and an isothermal plasma), which were kindly done at our request by R. Stern and R. Harnden, we estimate that >90% of the total X-ray luminosity accessible to *Einstein* falls within the 0.15–4.0 keV band, both for the early F stars and for the solar-type stars. If we adopt $T_{cor} = 10^{6.25}$ K for the F stars, then 92% of their X-ray flux is accounted for, and if we take $T_{cor} = 10^{6.5}$ K for the solar-type stars, then 97% of their flux is accounted for. Therefore, up to this step, we have no reason to question the X-ray deficiencies of the early F stars.

However, the same calculations also show that the low-temperature coronae of the early F stars may radiate approximately two-thirds of their emission at EUV energies below 100 eV, mostly in the Fe IX–Fe XI complex at ~70 eV, where the IPC instrument had no sensitivity. By comparison, the hotter coronae of the solar-type stars emit no more than 15% of their energy at EUV wavelengths. These results imply that the X-day deficits of the early F stars, at least those up to 0.45 dex, may be explained by the shift of much of their coronal emission to lower energies outside the *Einstein* bandpass. Whether or not the same can be said of the largest X-ray

deficits plotted in Figure 11, e.g., those of HR 3991 and β Cas, is unclear. If each X-ray deficit is reduced by 0.45 dex, there still remain 10 stars with deficits of at least a factor of 4. In the absence of direct EUV observations of these stars, the question can be settled only by a detailed analysis of the IPC pulse-height spectrum to determine the coronal temperature, X-ray flux, and EUV flux for each individual star. Unfortunately, as Schmitt *et al.* (1985*a*) noted, very few of the early F stars are strong enough X-ray sources to permit any sensible temperature analysis.

One exception to this statement is Procyon A, which was analyzed in detail by Schmitt *et al.* (1985*b*) and also by Jordan *et al.* (1986). Although we would not regard Procyon as an *early* F star, since its $B-V = 0.42$ makes it a borderline case, this star does have a very large X-ray deficit of 0.93 dex according to Table 5. Both studies made use of the same IPC observation, and from independent pulse-height analyses each group derived a low coronal temperature of 1.5×10^6 K. Procyon was also observed at EUV wavelengths by *EXOSAT*, which detected strong emission in the Fe complex at 70 eV. According to Jordan *et al.*, the EUV flux is entirely consistent with the soft X-ray flux measured by the IPC as well as the low T_{cor} implied by the latter, and is indeed the *major* contributor to the total coronal emissivity of Procyon. Notwithstanding this result, Jordan *et al.* also show that the coronal emission measure of Procyon (normalized to that of the chromosphere) is in fact smaller than that of the Sun by at least *an order of magnitude*.[6] If the low-temperature UV emission is distributed nonuniformly over the stellar disk, as Jordan *et al.* prefer, then the difference is even larger. Thus, the coronal structure of Procyon *does* seem to be very different from that of the Sun, even though its apparent X-ray deficit should not be taken at face value. Because there is as yet no reason to suppose that this result can be generalized to the early F stars, the combined X-ray and UV data of each star presumably need to be analyzed in as much detail as those of Procyon. This leaves us at an impasse, since, according to Schmitt *et al.* (1985*a*), the X-ray fluxes of all but a few of the A and early F stars are too weak for spectral analysis.

Despite this major uncertainty attached to the X-ray deficits of the early F stars, we believe it is worthwhile to speculate on the reasons why the coronae of the early F stars might be different from those of solar-type stars, since any such difference would have far-reaching consequences.

To explain the lack of correlation between C IV emission and stellar rotation at $B-V < 0.42$, WBS suggested that the chromospheres and transition regions of the early F stars may be heated by the shock dissipation of sound waves, rather than by the dynamo processes that operate in solar-type stars. This proposal is consistent with observations from *IUE* that show a peak in emission-line strength near spectral type F0 V, which corresponds to $B-V = 0.28$ and $T_{eff} = 7300$ K, the same location where theoretical calculations predict a maximum in the acoustic power available from stellar convection zones (Renzini *et al.* 1977; Gilliland 1985*a*).

Here we wish to speculate that the coronae of the early F stars are also heated by sound waves. We readily concede that this is unlikely to be true for the Sun, and by extension for other solar-type stars, since waves in the solar atmosphere seem to be dissipated in the very low chromosphere and therefore fail to reach coronal heights. Nevertheless, acoustic waves would appear to be a reasonable candidate for heating the outer atmospheres of the early F stars, since the UV emission lines and X-ray flux of these stars are all uncorrelated with rotation. Acoustic waves would have no difficulty in meeting the energy requirements imposed by the observed UV and X-ray luminosities of the F stars, even though the mechanical flux predicted by mixing-length models for such thin convection zones may be uncertain by many orders of magnitude (Fontaine, Villeneuve, and Wilson 1981; Sofia and Chan 1984), and despite similar doubts about the theory that describes how such waves can propagate to coronal heights (Renzini *et al.* 1977; Ulmschneider *et al.* 1977).

Moreover, in our view, a very plausible explanation for the reduced X-ray emission of the early F stars is that the coronae of these stars, driven by thermal pressure gradients or by the acoustic waves, are undergoing expansion and that this expansion lowers the coronal emission measure and flux. If there are no large-scale magnetic fields to couple these coronal winds to the star itself, as we presume, then the generally rapid rotation of these stars is understandable. On the other hand, were we to propose an analogy between the atmospheres of the early F stars and solar coronal holes, we could not meet this objection, since the large-scale open fields in coronal holes would have a strong rotational braking effect. Rather, it is the sudden onset of dynamo action in main-sequence stars at spectral type F5 near $B-V = 0.42$, as indicated by the first signs of a rotation-activity correlation, that marks the first point at which stellar dynamos can generate strong surface magnetic fields, including a magnetized wind. Thus, it is within a few hundredths of a magnitude in $B-V$ color that main-sequence stars develop the capacity for magnetic braking. As far as we are aware, this abrupt cutoff in acoustic heating and growth in the strength of the dynamo is unexplained by theory. Similarly unexplained by theory is the sudden demise of activity and rotation among the evolved subgiants near $B-V = 0.6$, which we also attribute to the onset of stellar dynamos. The somewhat later spectral type at which this occurs for the subgiants, and the relatively larger X-ray deficits that they have when compared with main-sequence stars, is perhaps due to a much greater mass-loss rate.

Our interpretation of the early F stars differs from that of previous workers (e.g., Kraft 1967; Durney and Latour 1978) who thought that these stars supported insignificant winds once they arrived on the main sequence. Skumanich and Eddy (1981), for example, proposed that stellar magnetic fields undergo a transfiguration at spectral type F5 V from fields that are predominantly closed (bipolar) in the early-type stars to fields having both open (unipolar) and closed configurations in the later type stars. The closed magnetic fields of the warm stars would thereby generate strong chromospheric and coronal activity but not a powerful rotational brake. Were that the case, we would expect to find $N_R \ll 1$ rather than $N_R > 1$ for the early F stars, and we would further expect their UV emission to be strongly correlated with rotation (since the distribution in $v \sin i$ for these stars is consistent with a true spread in v_{eq}, not just in $\sin i$). However, neither expectation is met.

At the same time, we acknowledge a potential difficulty with our scenario of acoustic heating, which again concerns the "borderline" case of Procyon. According to Jordan *et al.*

[6] The theoretical total radiative power-loss function, $P(T)$, is relatively insensitive to temperature near 10^6 K, increasing by approximately a factor of 2 between $10^{6.2}$ and $10^{6.5}$ K (e.g., Rosner, Tucker, and Vaiana 1978). In terms of the total coronal radiation losses, this only partially offsets the factor of 10 reduction in Procyon's differential emission measure.

(1986), the nonthermal widths of the high-temperature UV lines of this star are just barely supersonic, which places very severe constraints on the energy flux that is carried by pure sound waves at transition region temperatures. We have no counterargument for their result. Rather, we suggest that a definitive test will be possible only with high signal-to-noise, high-dispersion line profiles that will become available for the early F stars from the Hubble Space Telescope (HST). The most conclusive test would be provided by observations of the UV coronal lines of these stars. A search for Doppler shifts in the forbidden lines of Fe XII at 1242 and 1349 Å, for example, might provide direct evidence of the coronal outflows that we believe may exist, and we encourage the guaranteed time observers using the Goddard High Resolution Spectrograph to look carefully for such effects.

IV. THE ACTIVITY OF COOL GIANT STARS

a) The Ultraviolet Emission of Giants

One of the first important achievements of *IUE* was the discovery of a "boundary line" among luminous stars in the cool half of the H-R diagram. Linsky and Haisch (1979) claimed to find a sharp dividing line near $V-R=0.8$ (approximate spectral type of K0) that separated the yellow giants, whose UV spectra showed evidence for chromospheres and transition regions, from the red giants, whose spectra showed evidence for chromospheres only. A similar "coronal dividing line" was found in X-ray data from *Einstein* near the same location, and extending up to the supergiants, by Ayres *et al.* (1981). Subsequent work has revised these ideas, suggesting that the dividing lines may not strictly apply to the bright giants or supergiants of luminosity classes I and II. Nor do they apply to rapidly rotating, synchronized binaries of the RS CVn class. According to Antiochos, Haisch, and Stern (1986), the existence of a coronal dividing line may be explained by instabilities that prevent the formation of hot coronal loops in stars of low surface gravity.

While the luminosity class III giants redder than $V-R=0.8$ apparently have much less plasma at transition region temperatures than do G giants, the picture is more complicated than the one originally portrayed by Linsky and Haisch (1979). In Figure 12 we have plotted the observations of C IV and C II emission for our sample of giants as a function of their $B-V$ color. Because the distances and absolute magnitudes of these high-luminosity stars are very uncertain, we have not tried to construct an H-R diagram for them as we did for the dwarfs and subgiants before. Both panels in Figure 12 show the following trends, which were also noted by Simon (1984) from a smaller sample of giants: (1) the early giants just entering the blue edge of the Hertzsprung gap[7] have very intense transition region emission lines; (2) the emission reaches an apparent peak among the early G giants near $B-V=0.7$; (3) with increasing $B-V$, the line strengths fall to much lower levels near the Linsky-Haisch boundary line; and (4) among the early K giants adjacent to the boundary line there is a very large spread in activity. We see no sign of a sudden decrease in emission near G5 III ($B-V=0.9$), at the location of Gray's

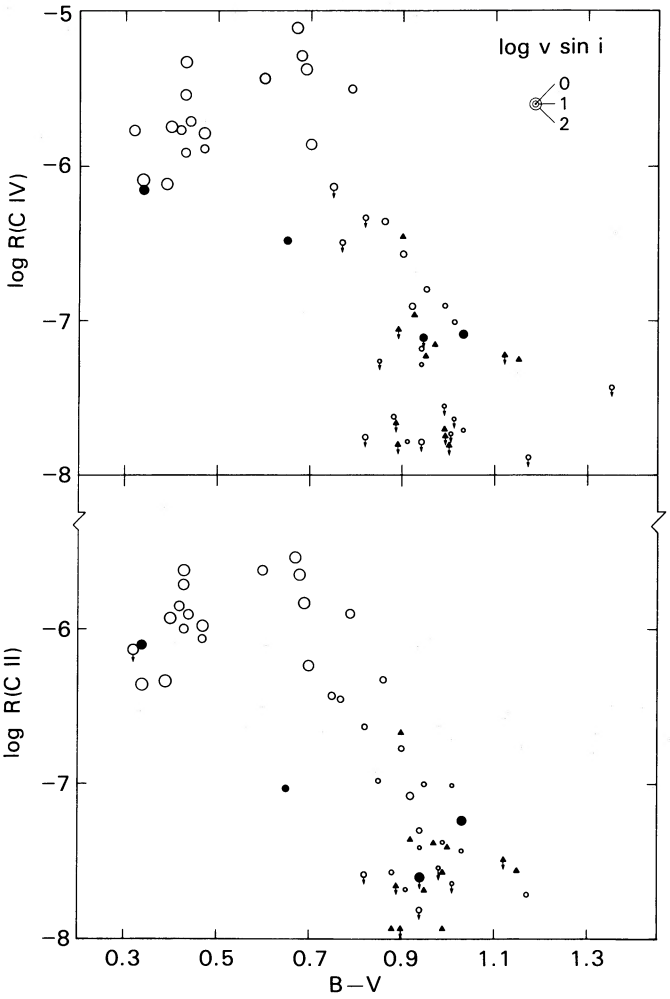

FIG. 12.—Normalized UV line fluxes for cool giant stars as a function of $B-V$ color for C IV (*top panel*) and C II (*bottom panel*). Stars of known rotational velocity are represented by circles whose size is proportional to v sin i. Filled circles denote upper limits on v sin i, and the triangles represent stars of unknown rotational velocity.

(1982*a*) "rotational boundary line." Rather, the falloff in UV emission across the Hertzsprung gap matches the gradual decline in rotational velocity that is present in the lower half of Figure 1.

It is generally believed that the chromospheric and coronal activity of late-type giants is largely due to magnetic dynamo activity, except possibly for a weak "basal" flux, which may show up in the low-temperature chromospheric emission of the most slowly rotating stars and which may be due to acoustic heating (Schrijver 1987). Thus, the falloff in activity with $B-V$ that Figure 12 reveals is presumably caused by a decline in dynamo activity across the H-R diagram. The acoustic flux generated by convection in low-gravity stars is also predicted by theory to decline with decreasing temperature (Renzini *et al.* 1977; Gilliland 1985*a*), but the change with $B-V$ is much too slow to be consistent with the steep falloff we actually observe.

A strong argument might be made in favor of the dynamo model if a correlation could be found between the strengths of the chromospheric and coronal emissions and the rotation rates. A plot of the C IV and C II line flux (Fig. 13) shows the hoped-for correlation, at least for stars with v sin $i > 5$ km s^{-1}.

[7] The earliest giants in our sample are 15 Ori (F4+ III, $B-V=0.32$) and 16 Per (F2 III, $B-V=0.34$). High-temperature lines might also be present in the UV spectra of earlier giants, but would be difficult to detect against their bright photospheric spectra. A deep survey for UV emission in these early giants would be extremely valuable for determining the locus of the onset of chromospheric activity in such relatively massive, evolved stars.

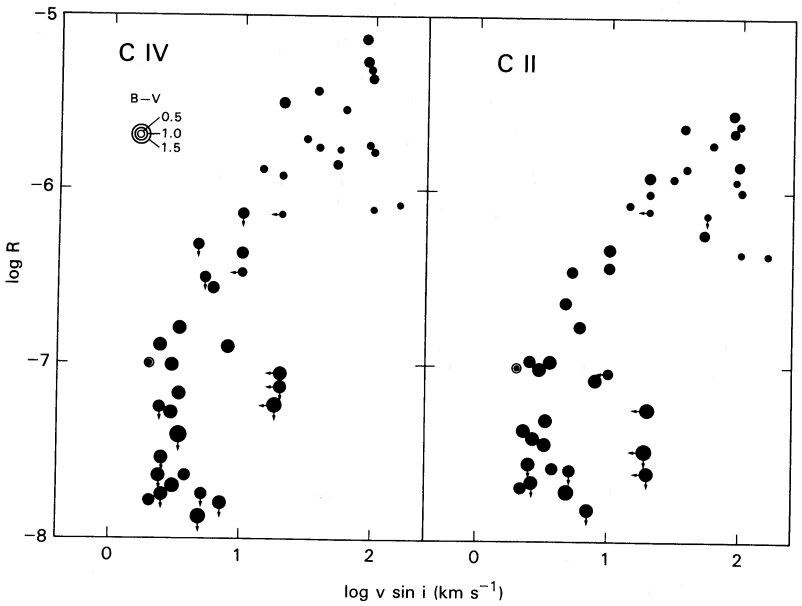

FIG. 13.—Normalized line flux for C IV (*left-hand panel*) and C II (*right-hand panel*) as a function of rotational velocity for late-type giants. The size of each symbol is keyed to the $B-V$ color index, with larger circles representing redder stars.

A formal least-squares calculation for the giants with normalized line strengths greater than 10^{-7}, which corresponds to the solar flux, yields the relations

$$\log R(\text{C IV}) = \underset{\pm 0.36}{-7.47} + \underset{\pm 0.11}{1.05} \log v \sin i \pm 0.07 ,$$

$$\log R(\text{C II}) = \underset{\pm 0.36}{-7.55} + \underset{\pm 0.10}{0.95} \log v \sin i \pm 0.07 .$$

(Of necessity, we ignore the six stars having only upper limits on their flux or rotation.) We note in passing that these relations are virtually identical to the ones that we derived earlier for the low-luminosity stars with $B-V \geq 0.42$, but this may be only a coincidence, since dwarfs, subgiants, and giants with the same rotation *period* have different R(C IV) strengths (Simon and Fekel 1987).

Thus, it appears from the foregoing analysis that the activity of the F and G giants with the brightest lines (or at least those with chromospheric and transition region emission above a certain threshold) may depend strongly on rotation and therefore originate from a dynamo. How, then, should one interpret the behavior of the most slowly rotating giants, whose weak fluxes show little dependence on rotation rate? A close examination of Figure 13 reveals a strong segregation according to $B-V$ color, in that the stars with the smallest fluxes and $v \sin i < 8$ km s^{-1} are also the coolest stars, which happen to lie next to the transition region boundary. The wide range in activity here (more clearly seen in C II than in C IV, as more than half of the C IV points are represented by upper limits) indicates that acoustic heating is probably not important for these stars, otherwise their emission ought to cluster near a minimum or basal flux level. Gray (1986) has suggested in his rotostat hypothesis that this dispersion might be due to "flickering" of a self-governing dynamo caused by repeated fluctuations or surges in activity that are then damped out by an enhanced magnetic braking effect. Such changes might well occur during stellar evolution near the base of the red giant branch as a star's convective envelope grows and acquires more rapidly rotating material from its radiative core (Endal and Sofia 1979).

While it is unclear to us why these interludes of strong activity should happen so intermittently, as Gray has said, instead of unfolding gradually over much longer evolutionary time scales, we believe the idea of feedback in his concept of the rotostat has considerable merit. Yet, whether such flickering occurs or not, Figure 13 suggests to us that at very slow rotation rates there is probably a steep, nearly vertical dependence of dynamo activity on rotation, which is easily obscured by systematic and random errors of only 0.5–1.0 km s^{-1} in $v \sin i$. If the giant stars follow a Rossby relation similar to the one established for the dwarfs, then at their large Rossby numbers—we estimate $N_R > 2$ for typical rotation speeds and with Gilliland's (1986) estimates of τ_c for a 2.5 $M_\odot$ star—their UV emission should drop off very sharply with increasing N_R. The present precision and accuracy of $v \sin i$ measurements may not be adequate to reveal this strong dependence.

b) Acoustic Heating in the Early Giant Stars

Since acoustic heating was suggested to be important for the late A and early F type dwarfs and subgiants at $B-V < 0.42$, can the same claim be made for the early-type giants, which also have thin convection zones? If one carefully inspects the flux versus $B-V$ plot in Figure 12, the giant stars with spectral types earlier than about F6, i.e., those with $B-V < 0.5$, all cluster together within a narrow range of activity in C IV and C II. In Figure 13 they appear embedded within the middle of the log R–log $v \sin i$ plots. A least-squares calculation for the 11 stars in this group yields the following regression for C IV:

$$\log R(\text{C IV}) = \underset{\pm 0.24}{-5.71} - \underset{\pm 0.82}{0.04} \log v \sin i \pm 0.47 ,$$

which implies that the activity of these stars is independent of rotation rate, just as we determined for the early F IV and F V stars. However, our sample of F giants is quite small, and a few of the luminosity classifications may be erroneous. Among the

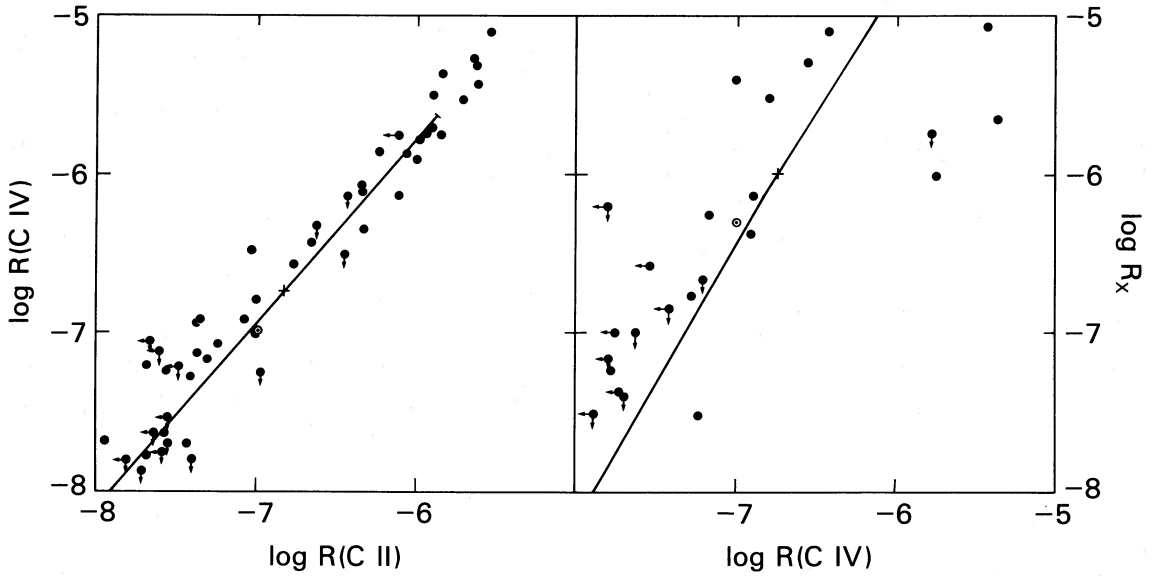

FIG. 14.—Flux-flux plots for giant stars. The position of the quiet Sun is indicated by the circled dot (as observed) and by the small cross (as expected according to its N_R). The solid lines are the Rossby relations for solar-type dwarfs.

early F stars, it is notoriously difficult to differentiate between low-mass stars of luminosity class IV and high-mass stars of class III, since the evolutionary tracks of these groups are not widely separated in luminosity (see Houk and Fesen 1978). For spectral classification we have tried to achieve some measure of consistency by relying upon the classifications assigned by no more than one or two spectroscopists. Since the most extensive work on our sample has been published by Cowley (e.g., Cowley 1976; Cowley and Bidelman 1979), we have given her classifications the highest weight. Nevertheless, a few of the early stars considered by us to be giants may yet turn out to be subgiants of lower mass. A more definitive assessment will require *IUE* observations for a larger group of F-type giants. Still, we point out that theoretical calculations for 2–5 $M_\odot$ stars do predict a peak in the acoustic flux for giant stars at spectral type late F or early G (Gilliland 1986, 1985*b*).

Flux-flux plots for the giant stars are presented in Figure 14. In the left-hand panel, all of the giants, even the F stars, fall along or lie close to the Rossby relation for the solar-type dwarfs, and so both groups have similar UV flux ratios. Very few of the giants have been observed at X-ray wavelengths. The X-ray observations we have taken from the literature, along with our own unpublished *Einstein* data, are plotted in Figure 8 as a function of $B-V$ color and in the right-hand panel of Figure 14 as a function of the normalized C IV flux. In the latter figure, the giants appear to be shifted above the Rossby relation of the solar-type stars, which would imply a higher X-ray flux for a given C IV flux. However, most of these measurements are upper limits rather than true detections.

Following the same steps that we used for the dwarf stars, we have determined the deviations of the X-ray measurements of the giant stars from the Rossby relation of the solar-type stars, i.e., we have determined the excess or deficit in X-ray emission corresponding to the observed C IV flux. (Stars with upper limits in UV emission have been ignored.) These deviations in X-ray flux, $\Delta \log R_X$, are shown in Figure 11, where they are plotted as plus signs. There are only three F-type giants for which we can make this comparison, and each is deficient in X-ray emission. This trio of stars includes the rapidly rotating F9 III secondary star of Capella,[8] which is thought to contribute most of the high-temperature emission observed from this binary (Ayres, Schiffer, and Linsky 1983). We also find an enormous X-ray deficit for the rapidly rotating G0 III star ψ^3 Psc. The *IUE* spectrum of this star displays very strong emission lines (Simon 1986), but ψ^3 Psc is at best a weak X-ray source. It was marginally detected by both *Einstein* (Simon 1986) and *EXOSAT* (Gondoin, Mangeney, and Praderie 1987); the two observations correspond to different energy bands but appear to be consistent with one another. We infer from these very large X-ray deficits that the coronal winds of the yellow giants just entering the Hertzsprung gap must involve a much higher mass-loss rate than those of the early-type subgiants and dwarfs. However, it is not until the giant stars evolve beyond the peak in UV emission among the early G stars and dynamo activity commences that these winds are able to act effectively to brake the rotation of the outer convective envelope. Yet, as we wrote in § I of this paper, it is a matter of continuing debate whether magnetic braking is truly important in this next phase of evolution or whether changes in the star's moment of inertia alone are able to explain the observed drop in rotation among the G giants (see, e.g., Endal and Sofia 1979; Gray and Endal 1982; Rutten and Pylyser 1988).[9]

Although we can say nothing here that would end that particular debate, we mention two other observations that seem relevant to our discussion of acoustic heating. First, in repeated observations with *IUE*, the active secondary component of Capella (Ayres 1984) and also ψ^3 Psc (Simon 1986) have both proved to be remarkably steady UV sources. Neither star has shown any evidence for the chromospheric inhomogeneities

[8] In this paper we have adopted the stellar and UV parameters of Capella from Ayres, Schiffer, and Linsky (1983). Use of the new parameters given by Ayres (1988*a*) and Bagnuolo and Sowell (1988) would lead to no significant changes in our results.

[9] Rutten's and Pylyser's discussion unfortunately misses the point that in order to determine whether angular momentum is conserved one must consider how the statistical distribution of $v \sin i$ changes during evolution across the H-R diagram. It is not enough just to show, as in their Fig. 2*a*, that the observed velocities of the late-type giants and their main-sequence progenitors fall within the same arbitrarily chosen upper and lower bounds.

often observed in *IUE* spectra of the equally rapidly rotating stars of the RS CVn class. The lack of variability, especially on time scales comparable to a rotation cycle, implies that the activity of both stars, Capella and ψ^3 Psc, is distributed rather widely and uniformly across the stellar surface, as one might expect if acoustic heating is involved. In fact, Ayres (1984) derived a surface coverage for Capella of >60% in C IV emission. By comparison, the C IV filling factor of the Sun at almost any point in its magnetic activity cycle is at least an order of magnitude smaller. And second, of the subgiants that show an X-ray deficit, only β Cas has been monitored for changes in its UV line flux, and this star also failed to show any signs of intrinsic variability (Ayres 1988*b*).[10]

c) The Radio and X-Ray Corona of Capella

At UV and X-ray wavelengths, Capella is one of the brightest stars in the sky, and it has long been considered the archetypal "active chromosphere" star. Yet radio observations of Capella have always found this star to be a surprisingly weak source. Compared with RS CVn stars of the same orbital or rotational period, for example, the 6 cm radio emission of Capella is nearly 100 times less than expected (Drake, Simon, and Linsky 1989). In a recent discussion of this problem, Drake and Linsky (1986) have pointed out that Capella's 6 cm radio flux is within a factor of 2 of the *thermal* emission one would expect from an optically thin radio corona having the emission measure implied by Capella's observed X-ray flux. On the other hand, the more powerful microwave emission of the RS CVn stars, even the low-level nonflare emission, is 10–100 times greater than the thermal emission one would predict from their X-ray flux. Their radio flux is generally considered to be gyrosynchrotron radiation from mildly relativistic electrons, which are spiraling in magnetic fields of 10–100 G. Thus, the faint radio emission of Capella may be entirely consistent with our view that the corona of this star is heated by sound waves instead of by the magnetic processes that take part in heating the corona of the Sun.

It is important to note here that the widths of the UV emission lines of the early-type star in Capella, unlike those of Procyon, which we discussed earlier, are extremely broad and highly supersonic (Ayres, Schiffer, and Linsky 1983; Ayres 1984, 1988*a*). If this broadening is due not to opacity effects and not to large-scale flows in the atmosphere but rather to wave motions, then a strong flux of acoustic energy may be finding its way up to the transition region and corona of this star. However, there is no hard spectroscopic evidence that either layer of the atmosphere is actually expanding outward in a wind. Ayres (1984, 1988*a*) has examined the *IUE* spectra of Capella very carefully for Doppler shifts in the emission lines and found that most of the lines appear redshifted. These Doppler shifts can be attributed to downdrafts in the transition region and chromospheric layers of the atmosphere. A few lines do exhibit a red asymmetry in their profiles, which could be a sign of outflows, but Ayres interprets these motions as the upward-moving leg of a global circulation pattern, the downflows being the return leg of this circulation flow. Much older spectra of O VI λ1032 acquired by the *Copernicus* satellite (Dupree 1975), seemed to indicate wind expansion in the transition region layers above 300,000 K, but there is some question now about which star in the Capella system and which orbital phase should be attached to these spectra.

X-ray spectroscopy was performed on Capella with the Focal Plane Crystal Spectrometer aboard the *Einstein* satellite (Vedder and Canizares 1983). Although emission lines of O VIII, Fe XVII, and Fe XX were detected, the signal-to-noise ratio of these observations was inadequate to demonstrate any blueshift of the emission lines from coronal wind expansion. HST observations of the UV coronal lines of Capella, as for Procyon, should settle this issue conclusively.

d) Rapidly Rotating Cool Giants

While the great majority of single, late-type giant stars rotate very slowly and exhibit only weak UV and X-ray emission, there is a growing list of stars that appear to violate the general rule. For example, Balona (1987) has recently identified eight early K giants in the southern hemisphere, all apparently single, that have moderate to fast rotation. In some cases, Balona estimates $v \sin i$ to be as high as 50 km s^{-1}. These unusual stars were first cataloged by Bidelman and MacConnell (1973) as having strong Ca II H and K emission cores, and each of them displays photometric variations attributable to starspots (Lloyd Evans and Koen 1987). *IUE* spectra were published by Simon and Fekel (1987) for two of these stars, HD 34198 (K0 III, $v \sin i = 15$, $P_{rot} = 28.4$ days) and HD 203251 (K2 III, $v \sin i = 40$, $P_{rot} = 44.3$ days). Several more examples are illustrated here in Figure 15. These UV spectra show an impressive array of high-temperature emission lines. The normalized C IV fluxes of these stars lie in the range (2–20) $\times 10^{-6}$, making these R(C IV) values at least 10 to more than 100 times larger than the R(C IV) of the "normal" early K giants plotted in Figure 12.

If one puts aside the rare, ultrarapid rotators of the FK

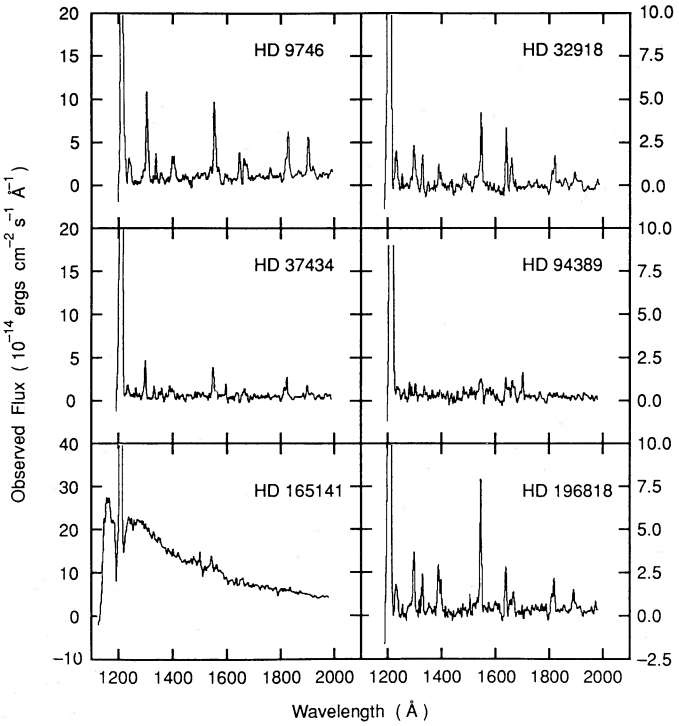

FIG. 15.—Low-resolution *IUE* spectra of six rapidly rotating, single K giants. These excellent archival spectra are guest observations made by F. C. Fekel.

[10] The star β Cas is a δ Scuti variable, but any short-term UV variability associated with its pulsation seems to be at, or below, the threshold of detection with *IUE* (Teays 1988).

Comae class, which may be the descendants of W UMa binaries whose components have merged (Bopp and Rucinski 1981), the evolutionary status of the rapidly rotating, single giants can be considered essentially unknown. In a few instances, after careful radial velocity measurements have been obtained, these single stars have turned out to be spectroscopic binaries with very low mass companions, e.g., the former FK Com candidate UZ Librae (K0 III, $v \sin i = 65$ km s^{-1}) is now known to be a single-lined spectroscopic double with an invisible $\sim 0.5\ M_\odot$ secondary (Bopp *et al.* 1984). A second example of a pseudo-single giant is HD 165141, whose *IUE* spectrum reveals the unmistakable imprint of a hot, subluminous companion (see Fig. 15). Balona estimated a relatively slow $v \sin i < 10$ km s^{-1} for the K0 II/IIIp primary star; however, the photometric rotation period of this star is $P_{\rm rot} = 34.6$ days (Strassmeier *et al.* 1988), which is substantially faster than the >100 days rotation periods we would expect for bona fide single K giant stars. In our view, HD 165141 is much like the similar nearly pole-on system AY Ceti, whose late-type primary now rotates asynchronously and is likely to be spinning down as it evolves up the giant branch.

A possible clue to the evolutionary status of these rapidly rotating giants has been provided by Fekel (1988), who has found a moderate or strong lithium absorption line in the spectra of each of these stars. A strong lithium line indicates that such stars may only recently have become giants (although in some cases the luminosity classification is itself suspect) and are in a stage prior to deep convective mixing on their first crossing of the H-R diagram. If these stars are indeed first-crossing stars, Fekel (1988) suggests that they may have evolved from rapidly rotating A stars. However, this explanation appears incomplete to us because the calculations of Endal and Sofia (1979) and Gray and Endal (1982), as well as Rutten and Pylyser (1988), all show that stars as massive as 5 $M_\odot$, which evolve conserving angular momentum, arrive at the base of the red giant branch with $v \sin i < 15$ km s^{-1}. For example, a 3 $M_\odot$ star that departs from the main sequence with twice the average rotational velocity, or 300 km s^{-1}, would still have a rotation speed <15 km s^{-1} as a K giant according to case 3 of Gray and Endal (1982), which maintains uniform specific angular momentum in convective regions. Thus, it would appear very hard to explain $v_{\rm eq}$ as high as the 50 km s^{-1} observed for HD 32918 or the 40 km s^{-1} observed for HD 203251 at K2 III.

As an alternative explanation, we would like to propose here that if these stars are truly in their first crossing, then their rapid rotation may stem from a sudden dredge-up of angular momentum from the interior. Given their $B-V$ colors, all of these stars are now situated along the red giant branch at a point where the outer convection zone is beginning to reach into deeper layers of the star. According to the models of Endal and Sofia (1979), up to this point such stars have been rotating differentially as they passed through the Hertzsprung gap; now they can entrain high angular momentum material from their cores on very short convective time scales. If this is the case, then the remaining slowly rotating, chromospherically inactive K giants must already have passed through this phase and already have been spun back down to much slower rotation rates (perhaps by a magnetic brake). Indeed, there is a high probability that most of the slowly rotating K giants are much older second-crossing stars (Simon 1984). Thus, it is in this quasi-static sense that we subscribe to Gray's idea of a rotostat, but one that does not "flicker."

V. SUMMARY

Our new *IUE* observations of late-type subgiants indicate that low-mass stars with $M < 1.25\ M_\odot$ experience neither a large increase nor a large decrease in activity once they leave the main sequence, at least not until they start their ascent of the red giant branch. That finding contradicts some earlier predictions of a resurgence in activity among cool subgiants, due to a large increase in the convective turnover time, but instead seems to confirm the suspicion of other investigators that stellar dynamos are very inefficient at slow rotation speeds. Admittedly, we have not explained the weak chromospheric and transition region emission, R(C IV) $\sim 10^{-8}$, of the giant stars adjacent to the Linsky-Haisch transition region boundary line, but these stars may be evolved, second-crossing stars of much higher mass (only stars with $M > 1.5\ M_\odot$ have blue loops in their evolutionary tracks).

Stars in the mass range 1.25–1.5 $M_\odot$ seem to evolve off the main sequence, carrying their high levels of activity with them for a short time afterward, but near spectral type G0 IV undergo an abrupt decay in activity at the same time that their rotation is decelerated. We interpret this "boundary line" in rotation and activity as the locus of the onset of the dynamo, a transformation from acoustic heating in the early F stars to the dynamo-driven activity of the solar-type stars. Evolutionary models for 1.5 $M_\odot$ stars that conserve angular momentum (e.g., Endal and Sofia 1979; Rutten and Pylyser 1988) are unable to explain such a rapid change in surface rotation rate just by altering the moment of inertia alone. Thus, in our view, the development of a dynamo induces a strong magnetic braking action in a (preexisting) wind, which—because of the very short time scales involved—must act only on the outermost layers of the stellar surface. To explain how these changes can occur on such short time scales raises some difficult theoretical questions. The sudden onset of the dynamo may require, for example, a critical mass or thickness of the convection zone, say 10% of the stellar radius. At the same time, we note that the long-term angular momentum loss of the Sun seems to depend more on the coupling effect of magnetic field stresses than on the mass flux per se (Pizzo *et al.* 1983), so that perhaps the field geometry in the $\sim$G0 subgiants is arranged so as to create the maximum amount of torque and hence yield the maximum effectiveness of the wind in rotational braking.

For giant stars of $M > 1.5\ M_\odot$, we tentatively suggest that a similar transformation takes place in the nature of chromospheric/coronal heating near spectral type G0 III. The subsequent decline of activity within the Hertzsprung gap is accompanied by a drop in rotation, but we see this as happening more gradually over the 1–25 Myr evolutionary time scale needed to pass through this part of the H-R diagram than does Gray, who adovcates a discontinuous change in rotation near G5 III. If the evolutionary change in activity and rotation is more gradual, as we prefer to believe, then it is still unclear whether stars conserve angular momentum in the gap or whether an external rotational brake is needed. Based on our study of the X-ray data for a tiny sample of F- and early G-type giants, we believe such stars may be losing considerable mass in coronal winds. If these winds suddenly become magnetized with the onset of the dynamo, then there could be ample opportunity for the rotation rates of first-crossing giants to spin down to the much slower values that typify cooler giants.

As difficult as it is to explain the *slow* rotation rates of the vast majority of K giants, it is equally difficult to explain how

nearly a dozen early K giants, all of them apparently single, can have rotation rates >20 km s^{-1}. We have speculated that these stars may be first-crossing stars that have just entered a phase of rapid spin-up as their convection zones advance upon more rapidly rotating regions in the radiative core of the star. As a result, their activity has temporarily adjusted itself to a much higher level, and these stars should now undergo a stronger rotational wind-braking effect, which will act to damp out these higher levels of activity and rotation. This is an example of feedback in the magnetic dynamo.

Perhaps the most controversial aspect of this paper concerns our speculation that acoustic waves play a dominant role in heating the coronae, and possibly the chromospheres and transition regions, of the early F stars from dwarfs to giants. This is based on our consideration of their X-ray emission (which we assert to be weak relative to that of solar-type stars) and the relationship between activity and rotation (which we find to be uncorrelated, in contradistinction to the tight correlation exhibited by solar-type stars). We do not believe that an alternative model of a low-temperature ($\sim 2 \times 10^6$ K), low-density coronal hole would be appropriate for the early F dwarfs, since we would not then be able to explain their generally rapid rotation. This rapid rotation persists up to a much later point in time, even after these stars have left the main sequence (Danziger and Faber 1972; Gray and Nagar 1985), than can be reconciled with any arguments based on characteristic spin-down times, such as those made by Durney and Latour (1978). Nor do we feel it is appropriate to contend that F star coronae are shut off from their winds (by a closed magnetic field geometry), since we would then expect to see a very strong correlation between activity and rotation, which is contrary to our actual findings. We have suggested several future tests of this idea of acoustic heating, and we await the outcome of those tests.

We thank Dr. Yoji Kondo and the staff of the *IUE Observatory* for their assistance in the acquisition and reduction of the UV data presented here. Special thanks go to Rosalie Ewald for her help on numerous occasions at the Goddard RDAF. We also wish to thank Dr. F. D. Seward for supplying us with the *Einstein* archival data, and we are grateful to Dr. R. A. Stern and Dr. F. R. Harnden for undertaking the calculations we needed to interpret these observations. This research was supported in part by NASA grants NAG 5-146 and NAG 8419 to the University of Hawaii.

APPENDIX

DOUBLE REGRESSION

In this appendix we present our double regression method for fitting a straight line $y = a + bx$ to observational data when both variables y and x are subject to error. This problem has a long history, going back more than 100 years in the statistics and economics literature. Franklin (1960, p. 85) cites without attribution the best-fitting line for the case of equal errors in (all) y and (all) x. Franklin's solution is known as the orthogonal regression line because of the common, though erroneous, assumption that the best-fitting line is the one that minimizes the sum of the squares of the deviations normal to the line (see, e.g., Wald 1940). To our knowledge, the solution for the general case of unequal errors in y and x is originally due to Lindley (1947), with further discussion by Madansky (1959). These results, with some minor revisions, are derived here *ab initio* using mathematics more familiar to astronomers, and in addition we provide estimates for judging the quality of the fit. Discussion of a more general class of least-squares problems can also be found in Peterson and Solensky (1988, Appendix B).

In our formulation we assume that the observational uncertainty may differ from one data point y_j, x_j to the next, but the error in each x_j is a constant fraction λ of the error in y_j. Thus, if the error in y_j is ϵ_j, then the error in the paired x_j is $\lambda\epsilon_j$. Although the observational errors may be unknown *a priori*, we assume their ratio λ is known or can be estimated beforehand.

Following the standard approach outlined in almost any statistics textbook, we obtain a pair of least-squares normal equations by minimizing the χ^2 statistic,

$$\chi^2 = \sum_{j=1}^{N} \frac{(y_j - a - bx_j)^2}{\epsilon_j^2 + b^2(\lambda\epsilon_j)^2} ,$$

with respect to both of the unknown coefficients a and b. Taking the derivative of χ^2 first with respect to a and setting the result to zero, we recover the usual solution,

$$a = \bar{y} - b\bar{x} ,$$

where the overbar denotes the weighted average

$$\overline{(\ldots)} = \frac{\sum_j \epsilon_j^{-2}(\ldots)}{\sum_j \epsilon_j^{-2}} \equiv \sum_j w_j(\ldots)$$

and

$$w_j = \frac{\epsilon_j^{-2}}{\sum_j \epsilon_j^{-2}} .$$

Now taking the derivative of χ^2 with respect to the coefficient b and setting it to zero, we obtain the second minimization condition,

$$\sum_j w_j(y_j - a - bx_j)x_j + \frac{b\lambda^2}{1 + b^2\lambda^2} \sum_j w_j(y_j - a - bx_j)^2 = 0 .$$

After substituting the previous solution for a and collecting terms, we arrive at the following quadratic equation for the slope b:

$$b^2\lambda^2 + b\,\frac{(\overline{x^2} - \bar{x}^2) - \lambda^2(\overline{y^2} - \bar{y}^2)}{\overline{xy} - \bar{x}\bar{y}} - 1 = 0\,.$$

We next introduce the notation $v_x = \overline{x^2} - \bar{x}^2$, $v_y = \overline{y^2} - \bar{y}^2$, and $v_{xy} = \overline{xy} - \bar{x}\bar{y}$. These are, respectively, the variance of the observable x, the variance of the observable y, and the covariance of x and y. We also define the auxiliary parameter z,

$$z = \frac{v_x - \lambda^2 v_y}{2\lambda v_{xy}}\,.$$

The solution of the quadratic equation then yields two roots for b,

$$b_\pm = \frac{-z \pm \sqrt{1 + z^2}}{\lambda}\,,$$

corresponding to two different regression lines. Note that according to the solution derived above, $a = \bar{y} - b\bar{x}$, there are also two choices for a (a_+ and a_-), which correspond to the two roots of the quadratic equation in b. With only a slight change of notation, these results are identical to those presented earlier by Lindley (1947) and by Madansky (1959).

The two independent regression lines, $y_+ = a_+ + b_+ x$ and $y_- = a_- + b_- x$, should not be confused with the conventional least-squares solutions for y upon x (assuming x is error-free) and x upon y (assuming y is error-free), nor are they simple averages of these solutions. Rather, the conventional solutions correspond to the limiting cases $\lambda = 0$ and $\lambda \to \infty$.

Although in most cases it will be transparent from the context whether y_+ or y_- is the appropriate best-fitting line, one can also derive quantitative estimates for the goodness of fit to assist in the choice, as we will now show. We first write, as an estimate of the uncertainty in the value derived for the coefficient b,

$$\sigma_b^2 = \sum_j \left[\left(\frac{\partial b}{\partial y_j} \right)^2 \epsilon_j^2 + \left(\frac{\partial b}{\partial x_j} \right)^2 \lambda^2 \epsilon_j^2 \right].$$

It is a simple matter to show that

$$\frac{\partial b_\pm}{\partial y_j} = \mp \frac{b_\pm}{\sqrt{1 + z^2}} \frac{\partial z}{\partial y_j}$$

and also, from the definition of z, that

$$\frac{\partial z}{\partial y_j} = -\frac{\lambda}{2v_{xy}} \frac{\partial v_y}{\partial y_j} - \frac{z}{v_{xy}} \frac{\partial v_{xy}}{\partial y_j}\,.$$

To evaluate its derivative, we expand v_y explicitly in terms of sums:

$$\frac{\partial v_y}{\partial y_j} = \frac{\partial}{\partial y_j} \left[\sum_i w_i y_i^2 - \left(\sum_i w_i y_i \right)^2 \right] = 2w_j(y_j - \bar{y})\,,$$

and similarly, for the derivative of the covariance v_{xy}, we obtain

$$\frac{\partial v_{xy}}{\partial y_j} = w_j(x_j - \bar{x})\,.$$

We insert these three expressions for the derivatives of z, v_y, and v_{xy} into the equation for the derivative of b to derive

$$\frac{\partial b_\pm}{\partial y_j} = \pm \frac{b_\pm}{\sqrt{1 + z^2}} \frac{w_j}{v_{xy}} [\lambda(y_j - \bar{y}) + z(x_j - \bar{x})]\,,$$

and, proceeding in a similar fashion, we also have

$$\frac{\partial b_\pm}{\partial x_j} = \pm \frac{b_\pm}{\sqrt{1 + z^2}} \frac{w_j}{\lambda v_{xy}} [\lambda z(y_j - \bar{y}) - (x_j - \bar{x})]\,.$$

We now introduce these derivative terms into the expression for σ_b^2 given above, to find

$$\sigma_b^2 = \frac{b_\pm^2}{v_{xy}^2} \sum_j \epsilon_j^2 w_j^2 [\lambda^2(y_j - \bar{y})^2 + (x_j - \bar{x})^2]\,.$$

Defining $W = \sum_j \epsilon_j^{-2}$, we arrive at our final result for the uncertainty in the coefficient $b_\pm$:

$$\sigma_b^2 = \frac{b_\pm^2}{v_{xy}^2} \frac{\lambda^2 v_y + v_x}{W}\,.$$

For the uncertainty in a we write,

$$\sigma_a^2 = \sum_j \left[\left(\frac{\partial a}{\partial y_j} \right)^2 \epsilon_j^2 + \left(\frac{\partial a}{\partial x_j} \right)^2 \lambda^2 \epsilon_j^2 \right] .$$

The derivatives of a are evaluated from the solution of the normal equation, viz.,

$$a_\pm = \bar{y} - b_\pm \bar{x} = \sum_j w_j y_j - b_\pm \sum_j w_j x_j ,$$

which yields, for both the "positive" and "negative" regression lines,

$$\frac{\partial a}{\partial y_j} = w_j - \bar{x} \frac{\partial b}{\partial y_j} ,$$

$$\frac{\partial a}{\partial x_j} = -b w_j - \bar{x} \frac{\partial b}{\partial x_j} .$$

After some tedious but uncomplicated arithmetic, we arrive at our final expression for the uncertainty in a:

$$\sigma_a^2 = \frac{1 + b^2 \lambda^2}{W} + \bar{x}^2 \sigma_b^2 ,$$

where the plus and minus signs corresponding to the two quadratic roots are implicitly understood.

Last, as a measure of the overall quality of the least-squares fit, we write the standard deviation with complete generality as

$$s^2 = \frac{1}{N-2} \sum_j (y_j - a - b x_j)^2 \epsilon_j^{-2} (1 + b^2 \lambda^2)^{-1} \Big/ \frac{1}{N} \sum_j \epsilon_j^{-2} (1 + b^2 \lambda^2)^{-1} = \frac{N}{N-2} (b^2 v_x - 2 b v_{xy} + v_y) .$$

Again, there are two values of s, which correspond to the two independent (+ and −) solutions.

To evaluate the solutions of the double regression method and to compare its results with those of the conventional least-squares approach, we have written a menu-driven computer program for an IBM personal computer. The program is written in the BASIC language and runs under the DOS operating system. Copies of the program will be made available upon request.

REFERENCES

Alschuler, W. R. 1975, *Ap. J.*, **195**, 649.
Antiochos, S. K., Haisch, B. M., and Stern R. A. 1986, *Ap. J. (Letters)*, **307**, L55.
Ayres, T. R. 1984, *Ap. J.*, **284**, 784.
———. 1988*a*, *Ap. J.*, **331**, 467.
———. 1988*b*, private communication.
Ayres, T. R., Linsky, J. L., Vaiana, G. S., Golub, L., and Rosner, R. 1981, *Ap. J.*, **250**, 293.
Ayres, T. R., Marstad, N. C., and Linsky, J. L. 1981, *Ap. J.*, **247**, 545.
Ayres, T. R., Schiffer, F. H., III, and Linsky, J. L. 1983, *Ap. J.*, **272**, 223.
Bagnuolo, W. G., Jr., and Sowell, J. R. 1988, *A.J.*, **96**, 1056.
Baliunas, S. L., *et al.* 1983, *Ap. J.*, **275**, 752.
Balona, L. A. 1987, *South Africa Astr. Obs. Circ.*, No. 11, p. 1.
Barnes, T. G., and Evans, D. S. 1976, *M.N.R.A.S.*, **174**, 489.
Basri, G. 1987, *Ap. J.*, **316**, 377.
Bidelman, W. P., and MacConnell, D. J. 1973, *A.J.*, **78**, 687.
Bopp, B. W., Goodrich, B. D., Africano, J. L., Noah, P. V., Meredith, R. J., Hunt Palmer, L., and Quigley, R. J. 1984, *Ap. J.*, **285**, 202.
Bopp, B. W., and Rucinski, S. M. 1981, in *IAU Symposium 93, Fundamental Problems in the Theory of Stellar Evolution*, ed. D. Sugimoto, D. Q. Lamb, and D. N. Schramm (Dordrecht: Reidel), p. 177.
Cowley, A. P. 1976, *Pub. A.S.P.*, **88**, 95.
Cowley, A. P., and Bidelman, W. P. 1979, *Pub. A.S.P.*, **91**, 83.
Danks, A. C., and Lambert, D. L. 1985, *Astr. Ap.*, **148**, 293.
Danziger, I. J., and Faber, S. M. 1972, *Astr. Ap.*, **18**, 428.
Demarque, P., and Guenther, D. B. 1986, in *Lecture Notes in Physics 254, Cool Stars, Stellar Systems, and the Sun*, ed. M. Zeilik and D. M. Gibson (New York: Springer-Verlag), p. 187.
Drake, S. A., and Linsky, J. L. 1986, *A.J.*, **91**, 602.
Drake, S. A., Simon, T., and Linsky, J. L. 1989, *Ap. J. Suppl.*, in press.
Dupree, A. K. 1975, *Ap. J. (Letters)*, **200**, L27.
Durney, B. R., and Latour, J. 1978, *Geophys. Ap. Fluid Dyn.*, **9**, 241.
Endal, A. S. 1981, in *Solar and Stellar Magnetic Fields: Origins and Coronal Effects*, ed. J. O. Stenflo (Dordrecht: Reidel), p. 493.
Endal, A. S., and Sofia, S. 1979, *Ap. J.*, **232**, 531.
Fekel, F. C. 1988, *A Decade of UV Astronomy with the IUE Satellite*, ESA SP-281, Vol. **1**, p. 331.
Fontaine, G., Villeneuve, B., and Wilson, J. 1981, *Ap. J.*, **243**, 550.
Franklin, P. 1960, in *Fundamental Formulas of Physics*, Vol. **1**, ed. D. H. Menzel (New York: Dover).
Gilliland, R. L. 1985*a*, *Ap. J.*, **299**, 286.
———. 1985*b*, private communication.
———. 1986, *Adv. Space Res.*, **6**, 183.
Gilman, P. A. 1980, in *Lecture Notes in Physics 114, IAU Colloquium 51, Stellar Turbulence*, ed. D. F. Gray and J. L. Linsky (New York: Springer-Verlag), p. 19.
———. 1983, *Ap. J. Suppl.*, **53**, 243.
Gilman, P. A., and DeLuca, E. E. 1986, in *Lecture Notes in Physics 254, Cool Stars, Stellar Systems, and the Sun*, ed. M. Zeilik and D. M. Gibson (New York: Springer-Verlag), p. 163.
Glatzmaier, G. A. 1985, *Geophys. Ap. Fluid Dyn.*, **31**, 137.
Gondoin, P., Mangeney, A., and Praderie, F. 1987, *Astr. Ap.*, **174**, 187.
Gray, D. F. 1982*a*, *Ap. J.*, **262**, 682.
———. 1982*b*, *Ap. J.*, **261**, 259.
———. 1984, *Ap. J.*, **281**, 719.
———. 1986, *Adv. Space Res.*, **6**, 161.
Gray, D. F., and Endal, A. S. 1982, *Ap. J.*, **254**, 162.
Gray, D. F., and Nagar, P. 1985, *Ap. J.*, **298**, 756.
Gray, D. F., and Toner, C. G. 1986, *Ap. J.*, **310**, 277.
Hartmann, L., Hewett, R., Stahler, S., and Mathieu, R. 1986, *Ap. J.*, **309**, 275.
Herbig, G. H., and Wolff, R. J. 1966, *Ann. d'Ap.*, **29**, 593.
Hoffleit, D., and Jaschek, C. 1982, *The Bright Star Catalogue* (New Haven: Yale University Observatory).
Houk, N., and Fesen, R. 1978, in *IAU Symposium 80, The HR Diagram*, ed. A. G. Davis Philip and D. S. Hayes (Boston: Reidel), p. 91.
Howard, R., and LaBonte, B. J. 1981, *Solar Phys.*, **74**, 131.
Jordan, C., Ayres, T. R., Brown, A., Linsky, J. L., and Simon, T. 1987, *M.N.R.A.S.*, **225**, 903.
Jordan, C., Brown, A., Walter, F. M., and Linsky, J. L. 1986, *M.N.R.A.S.*, **218**, 465.
Kraft, R. P. 1965, *Ap. J.*, **142**, 681.
———. 1967, *Ap. J.*, **150**, 551.
———. 1970, in *Spectroscopic Astrophysics*, ed. G. H. Herbig (Berkeley: University of California Press), p. 385.
Lindley, D. V. 1947, *J. Roy. Stat. Soc. Suppl., Ser. B*, **9**, 218.
Linsky, J. L., and Haisch, B. M. 1979, *Ap. J. (Letters)*, **229**, L27.
Lloyd Evans, T., and Koen, M. C. J. 1987, *South African Astr. Obs. Circ.*, No. 11, p. 21.
Madansky, A. 1959, *J. Am. Stat. Assoc.*, **54**, 173.
Maggio, A., Sciortino, S., Vaiana, G. S., Majer, P., Bookbinder, J., Golub, L., Harnden, F. R., Jr., and Rosner, R. 1987, *Ap. J.*, **315**, 687.
Mangeney, A., and Praderie, F. 1984, *Astr. Ap.*, **130**, 143.
Noyes, R. W., Hartmann, L. W., Baliunas, S. L., Duncan, D. K., and Vaughan, A. H. 1984, *Ap. J.*, **279**, 763.
Oranje, B. J. 1986, *Astr. Ap.*, **154**, 185.

Peterson, D. M., and Solensky, R. 1988, *Ap. J.*, **333**, 256.
Pizzo, V., Schwenn, R., Marsch, E., Rosenbauer, H., Muhlhauser, K.-H., and Neubauer, F. M. 1983, *Ap. J.*, **271**, 335.
Renzini, A., Cacciari, C., Ulmschneider, P., and Schmitz, F. 1977, *Astr. Ap.*, **61**, 39.
Rosner, R., Tucker, W. H., and Vaiana, G. S. 1978, *Ap. J.*, **220**, 643.
Rucinski, S. M., and VandenBerg, D. A. 1986, *Pub. A.S.P.*, **98**, 669.
Rutten, R. G. M., and Pylyser, E. 1988, *Astr. Ap.*, **191**, 227.
Schmitt, J. H. M. M., Golub, L., Harnden, F. R., Jr., Maxson, C. W., Rosner, R., and Vaiana, G. S. 1985*a*, *Ap. J.*, **290**, 307.
Schmitt, J. H. M. M., Harnden, F. R., Jr., Peres, G., Rosner, R., and Serio, S. 1985*b*, *Ap. J.*, **288**, 751.
Schrijver, C. J. 1987, *Astr. Ap.*, **172**, 111.
Simon, T. 1984, *Ap. J.*, **279**, 738.
———. 1986, *A.J.*, **91**, 1233.
Simon, T., and Fekel, F. C. 1987, *Ap. J.*, **316**, 434.
Simon, T., Herbig. G. H., and Boesgaard, A. M. 1985, *Ap. J.*, **293**, 551 (SHB).
Simon, T., and Landsman, W. 1987, in *Lecture Notes in Physics 291, Cool Stars, Stellar Systems, and the Sun*, ed. J. L. Linsky and R. Stencel (New York: Springer-Verlag), p. 265.
Simon, T., Linsky, J. L., and Stencel, R. E. 1982, *Ap. J.*, **257**, 225.
Skumanich, A. 1972, *Ap. J.*, **171**, 565.
Skumanich, A., and Eddy, J. A. 1981, in *Solar Phenomena in Stars and Stellar Systems*, ed. R. M. Bonnet and A. K. Dupree (Boston: Reidel), p. 349.
Soderblom, D. R. 1983, *Ap. J. Suppl.*, **53**, 1.
Soderblom, D. R., Pendleton, J., and Pallavicini, R. 1989, *A.J.*, **97**, 539.
Sofia, S., and Chan, K. L. 1984, *Ap. J.*, **282**, 550.
Stauffer, J. R., Hartmann, L., Soderblom, D. R., and Burnham, N. 1984, *Ap. J.*, **280**, 202.
Strassmeier, K. G., Hall, D. S., Zeilik, M., Nelson, E., Eker, Z., and Fekel, F. C. 1988, *Astr. Ap. Suppl.*, **72**, 291.
Teays, T. 1988, private communication.
Ulmschneider, P., Schmitz, F., Renzini, A., Cacciari, C., Kalkofen, W., and Kurucz, R. 1977, *Astr. Ap.*, **61**, 515.
van de Kamp, P. 1954, *A.J.*, **59**, 447.
Vedder, P. W., and Canizares, C. R. 1983, *Ap. J.*, **270**, 666.
Vilhu, O. 1984, *Astr. Ap.*, **133**, 117.
Vogel, S. N., and Kuhi, L. V. 1981, *Ap. J.*, **245**, 960.
Wald, A. 1940, *Ann. Math. Stat.*, **11**, 284.
Walter, F. M. 1983, *Ap. J.*, **274**, 794.
Walter, F. M., and Linsky, J. L. 1986, *New Insights in Astrophysics: Eight Years of UV Astronomy*, ESA SP-263, p. 103.
Walter, F. M., and Schrijver, C. J. 1987, in *Lecture Notes in Physics 291, Cool. Stars, Stellar Systems, and the Sun*, ed. J. L. Linsky and R. Stencel (New York: Springer-Verlag), p. 262.
Weber, E. J., and Davis, L., Jr. 1967, *Ap. J.*, **148**, 217.
Wilson, O. C. 1963, *Ap. J.*, **138**, 832.
———. 1966, *Ap. J.*, **144**, 695.
———. 1968, *Ap. J.*, **153**, 221.
———. 1982, *Ap. J.*, **257**, 179.
Wolff, S. C., Boesgaard, A. M., and Simon, T. 1986, *Ap. J.*, **310**, 360 (WBS).

STEPHEN A. DRAKE: NASA/Goddard Space Flight Center, Code 602.6, UVSP-SMM, Greenbelt, MD 20771

THEODORE SIMON: Institute for Astronomy, University of Hawaii, 2680 Woodlawn Drive, Honolulu HI 96822